USF Tampa Graduate Theses and Dissertations   USF Graduate Theses and Dissertations

October 2021

Computer Simulation for Continuous Centrifugation of High-Density Cell Cultures

Hironori Tomizawa
University of South Florida

Follow this and additional works at: https://digitalcommons.usf.edu/etd

Part of the Biomedical Engineering and Bioengineering Commons

Scholar Commons Citation

Computer Simulation for Continuous Centrifugation of High-Density Cell Cultures

by

Hironori Tomizawa

A thesis submitted in partial fulfillment
of the requirements for the degree of
Master of Science in Biomedical Engineering
Department of Medical Engineering
College of Engineering
University of South Florida

Major Professor: Mark Jaroszeski, Ph.D.
Richard Heller, Ph.D.
William Lee, Ph.D.
Timothy Fawcett, Ph.D.

Date of Approval:
October 24, 2021

Keywords: COMSOL Multiphysics, Perfusion culture, Bioreactor

Acknowledgments

I appreciate all who supported me in completing the research and thesis. I appreciate Prof. Jaroszeski for advice on this research about bioreactor and centrifugal pumps. Although it was under COVID pandemic, we worked closely for several months. I appreciate committee member professors providing advice. I appreciate the Department of Medical Engineering and the College of Engineering for helping me in the process of completing this thesis. I also appreciate the COMSOL support team for CFD application operation and the collaborators in the biotechnology companies for giving me helpful advice.

Table of Contents

List of Tables

List of Figures

Abstract

Perfusion bioreactors are used for cell production for cell therapies. The system uses cell separation devices such as centrifuge to facilitate cell growth by separating cells and spent media and allows constant media replacement. However, current cell separation technologies can increase shear stress, are generally not continuous processes, and are not as efficient as desired. These limit the amount of media replaced per unit time. Therefore, there is a need for a new system or a method that operates continuously to minimize cell damage, yield high cell concentration, and exchange media effectively. A set of research questions was formulated: (1) develop a computer simulation model for the known cell concentrating dynamics of an industry-standard Centritech Lab III centrifuge as a semi-continuous device, (2) develop a model of a Centritech Lab III centrifuge for continuous operation, and (3) use a developed model to characterize cellular separation in two novel centrifuge designs with respect to feasibility.

Two types of models were made with COMSOL Multiphysics, (1) Centritech Lab III type models and (2) new continuous operation models. Study 1 modeled the throughput and efficiency of a Centritech Lab III. This model was tested with two different culture types: semi-continuous use in study 1-1 and fully continuous use in study 1-2. Study 2 simulated a new continuous operation model, and two new models were created in study 2-1. Theory-based assessment was performed in study 2-2. Flow velocity stability and shear rate were evaluated in study 2-3.

As a result, in study 1-1, a computer simulation model of a Centritech Lab III centrifuge as a semi-continuous device was developed. This model moved cells downward by centrifugal force and could increase cell concentration in the lower area of the bladder in a semi-continuous manner. In study 1-2, a Centritech Lab III centrifuge model for the continuous operation was developed. However, any tested flow settings couldn't carry the cells from the inlet to the exit stream, and it was found out that this system couldn't be adapted for continuous operation.

In study 2, a developed model was used to characterize cellular separation in two novel centrifuge designs with respect to feasibility. Two new models were created based on structure and media property tests: the OC model and the No-OC model. The OC model was challenging to increase the cell concentration, but based on the theory of $F_d = F_{cfg}$, adjusting flow velocity effectively reduced the possible cell stagnation. Some OC model test cases, considered supernatant removal, allowed removing a high volume of supernatant without losing many cells. The No-OC model yielded a greater cell concentration than the OC model and achieved high supernatant removal. These No-OC tests provided a possibility to use as a benchtop size continuous operation device, though it needed to consider additional cell collection devices. The flow velocity stability and the shear rate in the created model were assessed, and the high pressure and high shear rate were found in the narrow area of the models. Verification by computer simulation was considered to be meaningful.

Chapter 1: Introduction

1.1 Centrifuge Technology in Continuous Culture

CAR-T cell therapy is a cell therapy for cancer treatment that uses cultured high-density T cells to express the chimeric antigen receptor (CAR) in the patient body. T cells are extracted from collected patient blood. They are cultured and proliferated in the bioreactor to express the chimeric antigen receptor. Concentrated high-density CAR-T cells are injected back to the patient at each cell therapy session (Levine, 2016). Many different researchers have reported the success rate of this therapy, and for example, the complete remission rate in the several years' clinical trials was 70-94% reported by Wang (2017). FDA approved CAR-T therapy in the US in 2017.

Perfusion bioreactors are one of the continuous cell culture methods desired for producing living cells and cell-derived products for therapeutic applications, which now supports CAR-T cells and a variety of protein biologicals, vaccines, and cell therapies. The manufacturing process of T cells grows a large number and high density of cells continuously (10^7 cells/ml ~ 10^8 cells/ml) or semi-continuously, showing significant advantages compared to static batch culturing. High cell concentrations can be reached by the combination of rocking agitation and perfusion media exchange (Janas, 2015). Primary T cells are sensitive to shear stress. While keeping the culture aerated and cells in suspension, agitation rates are optimized to protect these cells from damage in bioreactors. Microgravity culture such as a high aspect ratio vessel (HARV) bioreactor is another technology to create

a low shear stress environment. Also, media perfusion needs to be appropriately controlled. The system retains and immobilizes the cells and constantly removes solids, cell debris, precipitated materials, soluble non-product substances, and supernatant to obtain a high amount of product and keep a good media condition to provide sufficient fresh media for cell growth. The technologies such as centrifuge, filtration (depth filters, tangential flow filtration, alternative tangential flow), and acoustic resonance are used for cell retention and media exchange to remove unnecessary substances supernatant fluid. Figure 1.1 is a schematic representation of the cell separation process: (1) media is fed from bioreactor to cell separation device, (2) cell separation device separates cells from the supernatant (spent media), (3) concentrated cells return to the bioreactor, (4) the supernatant is discharged from the system (if not reused), and (5) fresh media is mixed with cells before or after returning to the bioreactor.
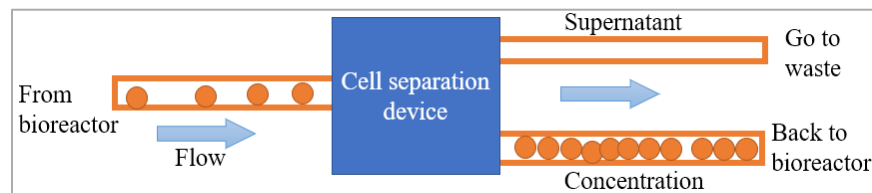
Figure 1.1 Cell separation in perfusion cultures.

Centrifuge technology is used in the several stages of the T cell production process to separate lymphocytes from other blood components and enrich the product's cell concentration by removing unnecessary substances. Perfusion culture can utilize a centrifuge device to separate cells from waste, which allows fresh media. Fresh media can then be added to the cells upon their return to the reactor so that they are not diluted. A centrifuge separates substances by weight using centrifugal force combined with gravity.

2

The basic structure of a centrifuge system is a rotating unit to apply the centrifugal force and a pump unit to feed cells in media and to remove concentrated cells and supernatant separately. There are several types of cell separation technologies currently in use. Dryden (2020) summarized the methods and introduced disk stack centrifugation and single-use centrifugation, such as counterflow elutriation. Disk stack centrifuge has multiple layers of a disk in the unit and has advantages such as high throughput, process high cell density, and low operating expenses. The disadvantages of disk stack centrifuges are that there are a limited number of bench-scale models, they require secondary clarification, infrastructure for clean-in-place (CIP) and steam-in-place (SIP) are needed, potential cell damage, high capital investment, and slow production. Shear stress potentially causes cell damage at higher flow rates, but lower flow rates increase cell lysis because of the longer residence time. The balance between centrifuge rotation speed and volumetric flow rate is critical to avoid impacting the cells (Shekhawat, 2018). Single-use centrifuges are benchtop size, and the sterilized unit is disposable. Centrifugation uses counterflow elutriation to separate lighter particles from heavier ones using a vertical stream of liquid. It has advantages that are low shear, no CIP and SIP systems, and fast product changeover. Disadvantages of single-use centrifugation are low throughput, nascent technology, low centrifugal forces, requires secondary clarification (Dryden, 2020).

Filtration has depth filters and microfiltration. Depth filters keep particles in a porous medium by retaining and absorbing soluble impurities. Depth filtration can remove soluble contaminants. Tangential flow filtration (TFF) and alternating tangential flow filtration (ATF) are the microfiltrations that use a peristaltic pump to recirculate the cell culture supernatant to the porous membrane surface. This process reduces the risk of stains

on the filter. In TFF, liquids and compounds with molecular weights smaller than the membrane cutoff can pass through the membrane, while larger molecules are retained. ATF uses TFF technology, but the diaphragm pump alternates the flow direction of the membrane surface. Microfiltration can operate over several days or continuously in perfusion, improve overall output and allow minimal secondary clarification. However, depth filters and microfiltration have low throughput when cell densities increase.

Acoustic resonance technology separates cells with high-frequency resonant ultrasonic waves instead of a physical mesh or membrane. Acoustic forces generate cell aggregates in the acoustic chambers. As more cells accumulate, they begin to aggregate and fall out of the solution by gravity. The cells are settled to the bottom of the chamber for continuous removal. It can operate for long-term cultivation without fouling or clogging (Applikon Biotechnology, n.d.). However, the separation throughput is one of the limitations of this technology (Wu, 2019).

Continuous culture processes are generally not large-scale mass production because from an industrial standpoint. Reactors are typically benchtop devices for culturing a batch of cells for days to weeks. Each retention technology has advantages and disadvantages, but increasing the density of cells and throughput were essential for cell therapy perfusion cultures. Therefore, centrifuge technology was selected in this research to enhance cell proliferation and combine the advantages of disk centrifuge and single-use centrifuge.

1.2 Centritech Lab Series Centrifuge

The Centritech Lab series (Pneumatic Scale Angelus, USA) is a commercially available centrifugation device for cell separation. It has a single-use bladder and features

a benchtop size rotor unit. The system consists of a centrifugal rotor, a 27-ml separation bladder, a peristaltic pump for feed, and a control unit (Pneumatic Scale Angelus, 2018). The centrifugal rotor unit is a truncated cone shape with diameters of approximately 16cm as top and 22cm as bottom, and 5cm as height as measured. It is not thermoregulated. The separation bladder has one inlet tube for feed and two outlet tubes for supernatant and concentrated cells (Figure 1.2).
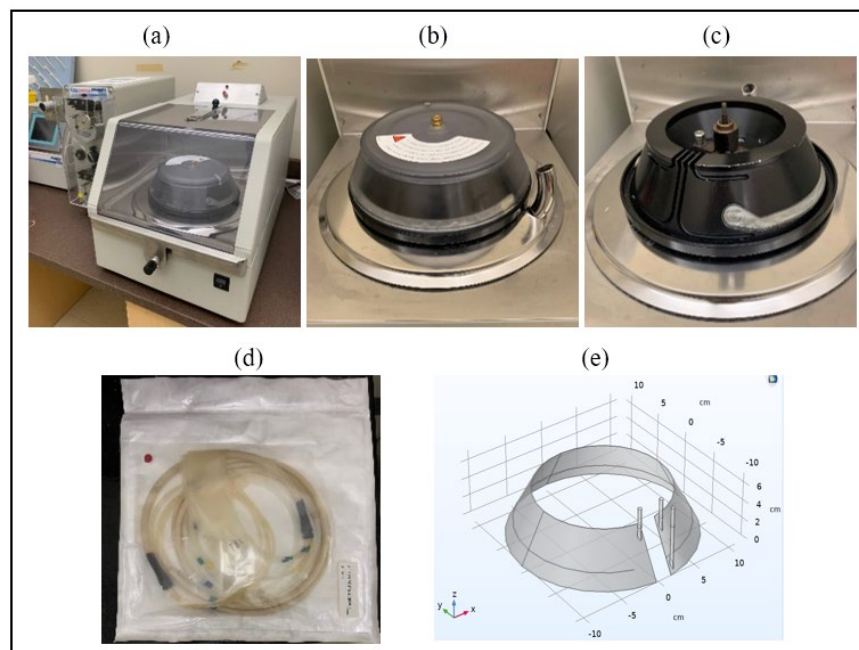
Figure 1.2 Centritech Lab III system and initial visualized 3D model.
(a) the external appearance of centrifuge unit, (b) rotor with a covering, (c) air barrier on the rotor surface, (d) sterilized bladder and tubes, (e) initial visualized 3D model in COMSOL.

The cell separation process in Centritech Lab III is unique and operated intermittently and semi-continuously. Each approach has a separation phase and discharge phase, and the patterns of phase control are programmable. Fluid is continuously flown from the inlet during the separation phase. An inflatable air barrier on the middle of the rotor can

inflate and deflate to separate the bladder to the upper and lower part by the program. The air barrier is not inflated in the separation phase. During the discharge phase, the barrier is inflated and physically isolates the lower layer with the sedimented cell-rich media from the upper supernatant layer. The outlet for concentration (OC) flows the cell-rich media out from the lower part of the bladder, while the supernatant is released and disposed of from the upper part of the bladder. These separation and discharge phases are alternated by the time programmed.

This Centritech Lab series has been used to harvest high-density cells as an industry-standard centrifuge device with the preferred feature of a single-use benchtop system. However, this system also has limitations that Kim (2008) reported their experience in the perfusion culture of rCHO cells. Kim experienced damaged cells accumulated in the bioreactor, worsening the perfusion rates and increasing the number of dead and damaged cells. It was concluded that the reasons for damages were due to shear stress from the pump and centrifugal force, exposure to the environment of oxygen limitation, and low temperature. Their observations were (1) repetitive damage was caused by shear stress when the system was operated in the intermittent or semi-continuous manner, (2) Oxygen feed was limited during centrifugation, nutrient depletion continued, increasing the number of dead and damaged cells, and (3) the culture temperature decreased with the non-thermoregulated system.

From Kim's report and this device's operation manner, if the flow had circulated continuously without using the default flow setting of intermittent (semi-continuous) mode, the concentrated cells could have exited the bladder before receiving an excessive shear

force for a long time. It was also speculated that low nutrition and temperature drop could be alleviated if there was a continuous media flow in the centrifuge unit.

1.3 Purpose of Research and Research Questions

Higher cell density (10^7 cells/ml $\sim 10^8$ cells/ml) is critical to rapidly increasing the number of cells in the T cell bioreactor. The one million cells per milliliter (10^6 cells/ml) have been a common starting point of T cell culture. Current technology has brought viable cell density for T cells to the level of ten million cells per milliliter (10^7 cells/ml). The high concentration of cells has been fostered by reducing the damaged cells and constant media replacement to accelerate the cell growth rate. However, the current cell separation technology seems to increase pressure upon the cells (shear stress) and prevent high cell concentration, limiting the amount of media that can be replaced per unit time. Therefore, there is a need for a system or a method that can separate cells from the liquid phase more efficiently with minimal shear force to grow cells to higher densities while replacing the media.

Devices and methods currently used for cell separation, such as the counterflow elutriation device and the Centritech device, use alternate operations in which separation of cells from supernatant is performed in a batch or semi-batch manner. However, it has been hypothesized that it would be more efficient for increasing production if the separation device performs separation and discharge simultaneously to maintain a constant concentration of cells and release of supernatant. This simultaneous separation and discharge are called a continuous operation.

In considering a suitable device for the continuous operation method, modification of the current device (Centritech Lab III) was considered and investigated. A new device was also investigated. A device capable of the continuous operation method requires at least one inflow for media and two or more outlets. One outlet is used to discharge enriched cells, and the other is for supernatant outflow. Thus, a minimum of three total entrances and exits are required. Counterflow elutriation devices can't be operated in a continuous manner because they have only had a total of two entrances/exits. However, the Centritech Lab III device has one inlet and two outlets. It was recognized that these could be used as a continuous device; this research examined this possibility. In addition, the feasibility of a new centrifuge device design was also investigated. Both options were modeled using computational fluid dynamics (CFD). CFD is an engineering tool to simulate and analyze phenomena, including fluid dynamics and complex bioprocess (Shekhawat, 2018). COMSOL Multiphysics was used for modeling and simulation testing, and the simulation test results were analyzed and evaluated quantitatively.

The Centritech type simulation model was created by referring to its physical dimensions to analyze the performance in a continuous operation method. When this new model was designed, the ideal features were benchtop size, high throughput, and low shear stress damage which combined the advantages from both disk centrifuge and single-use centrifuge. This research focused on maximizing the centrifuge efficiency to shed light on how higher cell concentration can be achieved without losing cells. The basis of achieving higher cell concentrations is to increase the efficiency of separating cells from the supernatant and remove the supernatant from media as much as possible.

For the reasons described above, a set of research questions were formulated.

(1) Develop a computer simulation model for the known cell concentrating dynamics of an industry-standard Centritech Lab III centrifuge as a semi-continuous device.

(2) Develop a model of a Centritech Lab III centrifuge for continuous operation.

(3) Use a developed model to characterize cellular separation in two novel centrifuge designs with respect to feasibility.

Evaluation of the Centrtitech Lab III device's potential separation and discharge performance in semi-continuous and continuous operation was also used as benchmark data for the new design addressed in that the new model achieves.

Chapter 2: Materials and Methods

2.1 Study Structure

Two types of models were made with COMSOL Multiphysics to achieve the research goals. The first type of model that mimicked a Centritech Lab III centrifuge was evaluated for throughput and efficiency. The model for this centrifuge was tested with two different types of operation: semi-continuous use in study 1-1 and fully continuous use in study 1-2 (both below). The performance results were used as a baseline for the second model. Study 2 investigated the second type of model that was a new continuous operation model. The device structure, specification, and variable parameters were evaluated, and new models were created in study 2-1. The throughput and efficiency with the theory-based tests were assessed in study 2-2. The flow velocity stability and shear rate were evaluated in study 2-3. The new continuous model had two shapes with and without an outlet for cell concentration (OC). The OC model had a discharge route structure collecting concentrated cells to the center of the rotor. In contrast, the No-OC model didn't have the structure and directly discharged cells from the separating chamber.

2.2 Materials

The materials for this research included computer simulation application, T cell and media characteristics information, and the Centritech centrifuge pump specification information. Computer simulation used COMSOL Multiphysics to solve equations arising

in mathematical modeling using the finite element method (FEM) and Lagrangian approach for fluid dynamics analysis. Physical characteristics of T cells and media from the literature were provided to COMSOL for simulations. Specification information about the Centritech Lab III centrifuge pump was used to simulate in study 1-1 and study 1-2; this information was obtained from the manufacturer's provided information about the device. Microsoft Excel and SPSS statistics applications were used to analyze the received data statistically.

2.2.1 COMSOL Multiphysics CFD Module

COMSOL Multiphysics is a FEM simulation application that solves partial differential equations (PDEs) in mathematical modeling. Modeling steps are defined geometries, material properties, meshing, the physics that solve the phenomena, and data analysis (COMSOL, 2020).

The COMSOL CFD module has various physics interfaces for momentum transport modeling, such as laminar and turbulent flow, multiphase flow, Newtonian and non-Newtonian flow, and particle tracking. There were two ways to describe the motion of fluid: the Lagrangian approach and the Eulerian approach. This research used the Lagrangian approach. It is a method of tracking a fluid particle and describing it as a function of the initial position and time of the particle. It marks an element of fluid in the initial stage (t = 0) and tracks the movement of that element over time by focusing on that element. It is convenient when formulating the equation of motion for particle tracking.

This research used three interfaces of COMSOL CFD module: multiphase mixture turbulent flow k-ε interface, the single-phase turbulent flow k-ε interface, and the particle tracking for fluid flow interface. Since the Reynolds numbers vary depending on the applied

flow velocity and the characteristics of the unique shape, the turbulent flow model was chosen instead of the laminar flow model. The turbulent flow k-ε interfaces for both single and multiphase flows use the Reynolds-averaged Navier–Stokes (RANS) equations. RANS calculates based on the continuity equation that takes the Reynolds average and the Navier-Stokes equation. It predicts the time-averaged or ensemble-averaged solution of flow that is entirely in the turbulent state. The turbulent effect on the model is minimized in the low Reynolds number field.

The multiphase mixture interface solves the dispersed multiphase flows, where the cells travel at their terminal velocity. This interface solves Navier-Stokes equations for the momentum of the mixture, calculates the pressure distribution, the velocity of the dispersed phase, and the dispersed phase volume fraction (VF). In this research, the dispersed phase represents the cell concentration. The VF for the dispersed phases was evaluated as the separation and discharge efficiency criteria.

The single-phase flow interface computes the velocity and pressure fields. The particle tracing interface computes the particle motion in a background fluid calculated in the flow interface. These two interfaces were mainly used in the preliminary and supplementary testing to multiphase mixture interface testing in this research.

2.2.2 Definition of Cell and Media

The simulation requires defining the characteristics of cells and media. Naïve T cell size is 5 to 7 μm in diameter, and the density of lymphocyte is 1.073 to 1.077 g/ml (Tasnim, 2018., Zipursky, 1976). The cell shape was defined as a spherical shape, and their diameter and density are 7×10^{-6} m and 1077 kg/m^3 in the model, respectively, using SI units (Table

2.1). Several types of fluid media such as DMEM, RPMI with or without fetal bovine serum (FBS) were used for cell culture. The characteristics of RPMI 1640 medium + 0% FBS were used for calculation in this research. The density is 999.3 kg/ m^3, and the viscosity is 0.733 × 10^{-3} Pa·s at 37°C (Poon, 2020).

Table 2.1 Definition of cell and media.

Naïve T Cell	Definition in this Model (SI Unit)	
	Diameter [m]	7×10^{-6} [m]
	Density [kg/m^3]	1077 [kg/m^3]
Fluid Media (RPMI, 0% FBS) at 37°C	Definition in this Model (SI Unit)	
	Density [kg/m^3]	999.3 [kg/m^3]
	Viscosity [Pa·s]	0.733×10^{-3} [Pa·s]

2.2.3 Evaluation Criteria

Measurement criteria have been set to measure the performance in studies 1-1, 1-2, 2-1, and 2-2. The performance of throughput and efficiency in each study model has been evaluated by the volume fraction of cells in the fluid, condensation rate, and lost cell rate.

(1) Volume fraction: Volume fraction (VF) φ_i is the ratio of volume V_i of a component in the mixture to the total volume of all components before mixing. In this research, the dispersed phase is equal to the cell concentration. The dispersed phase VF φ_d is the ratio of the volume V_d of cell components in the mixture to the total volume V_t of all parts before mixing. The dispersed phase volume fraction φ_d is given by

$$\varphi_d = \frac{V_d}{V_t}$$

and the continuous phase volume fraction φ_c is the remaining phase as the fluid except cells given by 1 - φ_d. The volume fractions for the dispersed phase are evaluated as the separation and discharge efficiency criteria in this research.

(2) Condensation rate: The condensation rate considers the volume ratio of OC and represents condensation efficiency. The VF is measured at the OC exit. The ratio is calculated by the VF at OC exit after centrifuge over the initial VF before centrifuge. OC exit was located at the center of the model in the OC tract model, and it was below the separation chamber in the No-OC tract model.

(3) Lost cell rate: The lost cell rate is the volume of cells going out from the outlet for supernatant (OS) over incoming cells from the inlet to evaluate the supernatant condition. When the flow to OC is low, the lost cell rate becomes high. The cell loss should be minimized. The retention rate is the ratio of existing cells in the initial total cells, calculated from the lost cell rate.

2.3 Centritech Type Culture Model in Study 1

Centritech Lab III has a circular truncated cone shape rotor, in which the smaller radius on top is 8cm and the larger radius is on the bottom is 11cm, and the height is 5cm as measured. The bladder has a volume of about 30ml. The thickness of this volume is approximately 1mm. It has three tubes of the inlet for feed (IN), the outlet for supernatant (OS), and the outlet for cell concentration (OC), and the diameter of the tube is 5mm.

The rotor has an inflatable air barrier that works as an interior wall at 8mm from the bottom. When the air barrier is inflated, it separates the bladder to the upper and lower part by the program. The lower layer has sedimented cell-rich media isolated from the upper supernatant layer. Also, as a specific design feature, the interior barrier wall doesn't divide a bladder completely. The portions above and below are slightly connected at the right end of the inflated balloon, allowing the fluid flow.

2.3.1 Multiple Centritech Type Models in this Research

Three Centritech type culture models were created with COMSOL Multiphysics following the physics of the actual rotor's revolution. They were (1) 2D flat model type A, (2) 2D flat model type B, and (3) 2D symmetry model, simulating the application of centrifugal force, gravity force, and other forces to the cells and fluid. The fluid came from the inlet and went out from two outlets.

There was a reason to choose multiple 2D models. The actual Centritech device has an asymmetric shape, and the internal air barrier on the rotor works as a variable separation wall when the sedimented cells are discharged from the concentration outlet. The 3D model was created first in the early stage of this study. However, the computation time was too long to solve the problems or repeat many tests. Even the 2D models sometimes required a long-time to compute. The simplified 2D models enabled the various types of tests and analyzed the dispersed phase volume fraction by time-dependent. Solving 2D problems instead of 3D had the benefit of reducing the computation time and avoiding convergence error. Since any single 2D model couldn't reproduce the phenomenon in the 3D shape, two different 2D concepts were considered in this research to complement the limitation of each 2D shape.

2.3.1.1 2D Flat Model Type A and B

2D flat models described the bladder that was cut-open to the rectangle shape (Figure 2.1). 2D flat models had an inlet on the left top corner, an outlet for supernatant (OS) on the right top, and an outlet for concentration (OC) on the left bottom. This flat rectangular shape focused on understanding how the dispersed phase was spread from the

inlet to two outlets. Therefore, the models neglected that the top length was longer than the bottom and could not express the depth (z-direction).
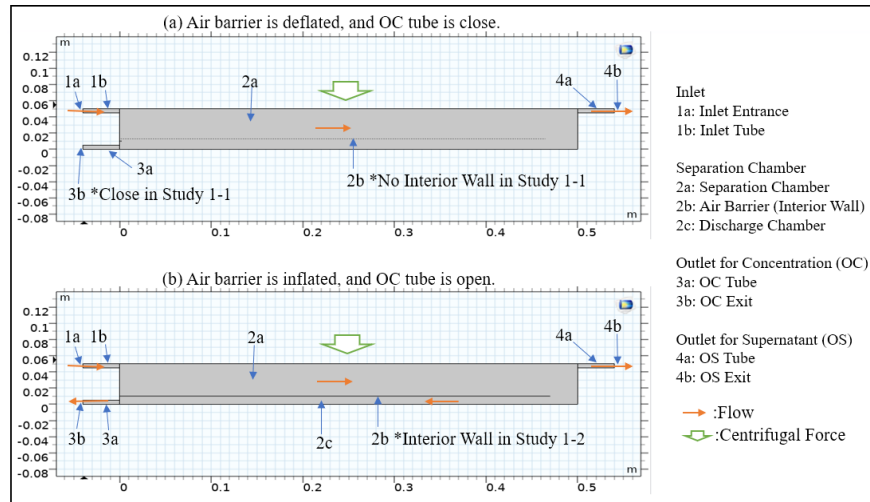
Figure 2.1 Centritech type culture 2D flat models.
(a) 2D flat model type A has deflated air barrier and closed OC tube, (b) 2D flat model type B has inflated air barrier and open OC tube.

The interior wall in model type A was disabled in study 1-1, and the whole area of the bladder was used as a separation chamber. However, the interior wall line was used only to measure the volume fraction of enrichment of the cells in the lower area. In contrast, the interior wall in model type B functioned as a solid wall in study 1-2. The flow branched off at the right end of the interior wall, and the flow to OC went under the interior wall. The specifications of the 2D flat models are as follows: bladder height 5cm, bladder length 50cm, the diameter of inlet and outlets 0.5cm, the interior wall height 0.8cm (from bottom), the interior wall length 47cm (from left).

Centrifugal force was converted to 2D toward the negative y-direction proportional to the distance from the center of the rotor. The closer to the bottom, the greater the centrifugal force because the shape was a truncated cone with an 8cm top radius and 11cm

bottom radius. When converting 3D to 2D, the following assumption was made. The centrifugal force generated on the rotor acts horizontally outward on the cells in 3D condition, but the cells are redirected by the surrounding wall and move diagonally downward according to the angle of the wall. The negative z component of the diagonally downward force vector generated in the 3D was expressed as the force used in the negative y-direction in this 2D model.

2.3.1.2 2D Symmetry Model

2D symmetry model described the axial symmetric rotor and bladder composed of the radial (r) and vertical (z) directions. This symmetry model aimed to measure how much the volume fraction of cells can be enriched in the bladder's lower area by centrifugation. This symmetric model factored the distance from the center of the rotation and bladder thickness but could not make a horizontal flow from inlet to outlets, unlike the 2D flat model.

The specifications of the 2D symmetry model were as follows: bladder height 5cm, bladder top radius 8cm, bladder bottom radius 11cm, the thickness of the bladder 1mm, the interior wall height 8mm (from bottom). The bladder volume was about 30 cm^3 (29.63 cm^3). The volume below the interior wall line was about 5 cm^3 (4.75 cm^3), becoming the area for discharging enriched cells (Figure 2.2).

2.3.2 Protocol for Study 1-1

Study 1-1 used 2D flat model type A and 2D symmetry models in the semi-continuous operation. The 2D symmetry model had two scenarios that found the highest centrifuge output by refilling the media.

17
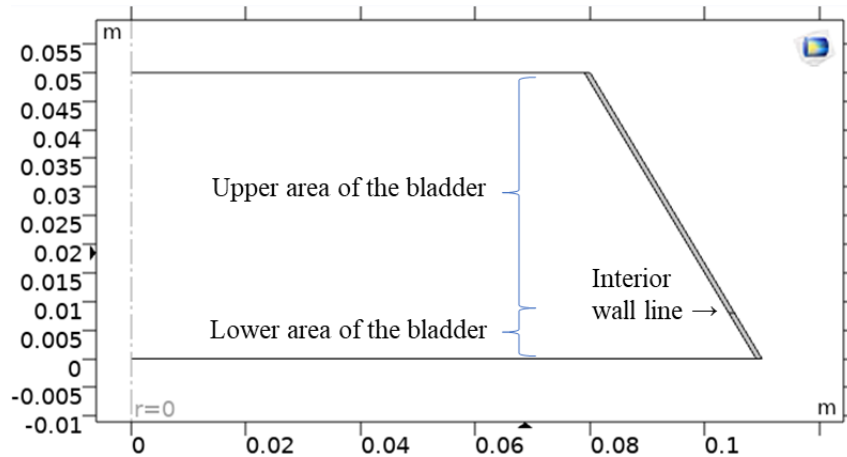
Figure 2.2 Centritech type culture 2D symmetry model.

2.3.2.1 2D Flat Model (Type A) Test

The 2D flat model test intended that the feed came from the inlet (IN) entrance on the top left, and the cells were moved downward by the applied centrifugal force while traveling in the bladder by the flow. Inlet flow velocity and centrifugal force were the given parameters. The supernatant exited the bladder from the OS exit on the top right (Figure 2.1a).

In the geometry setting, Centritech type 2D flat model type A was used. IN and OS were open. OC was closed, and an interior wall was not used. In the media setting, the initial VF of media was 1.8×10^{-3}. The inlet flow velocity in the inlet tube was set to 0.001, 0.01, 0.04, 0.08, and 0.16 m/s. (The flow velocity of 0.04 m/s was equivalent to the volume flow rate of 0.79 ml/sec, and 0.16 m/s was 3.14 ml/sec in the models of this study. The calculation of volume flow rate is in appendix B.) The number of disk rotations controls centrifugal force, and the range was 200, 600, and 1000 rpm. VF was measured at (1) OC exit and (2) averaged OC area in the lower chamber. Each simulation required 10 or 30 minutes until the VF increase became a plateau. A new simulation was started after flow and rotation speed were changed.

18

These were anticipated results.

- It would visualize how the vertical centrifugal force and the horizontal flow affect the distribution of the dispersed phase concentration in the bladder.

- The larger the centrifugal force, the larger the VF due to concentration.

- If the inlet flow was fast, the cell concentration would be diminished at the exit.

2.3.2.2 2D Symmetry Model Test

The 2D symmetry model simulation intended that the cells moved outward and downward by the applied centrifugal force. No inlet or outlets were modeled. Centritech type 2D symmetry model was another geometry dedicated to the separation and ignored the horizontal flow. This model didn't have an inlet and outlet on the geometry, but a virtual inlet was made on top to enable media refilling. Two scenarios were given for this test. Scenario #1 was no refilling of media during the simulation. Scenario #2 was that the media was refilled artificially, keeping the bladder's top in the initial condition as the inlet in the 2D flat model did.

The Initial VF of media was 1.8×10^{-3}. The number of disk rotations controlled centrifugal force, and the range was 100, 200, 600, 1000, and 2000 rpm. Each test was simulated for 10 or 30 minutes until the VF increase became a plateau. VF was measured at the averaged area in the lower chamber.

These were the anticipated result.

- The VF concentration in scenario #1 without refill would represent the case without being affected by the flow. For this case, it was expected that the VF below the

interior wall line would be enriched by centrifugation. The VF in locations far from the center would increase. The larger the centrifugal force, the larger the VF.

- The VF concentration with a refill in Scenario #2 would represent the case as if the inlet flow efficiently spread over the entire bladder. For this case, it was expected that the VF above the interior wall line represents the disposed supernatant, which must be small.

2.3.3 Protocol for Study 1-2

Centritech type culture model type B was simulated to determine the possibility of fully continuous operation in this study. The air barrier functioned as a solid interior wall. Inlet and both OS and OC were open to flow in and out. The distance that the cells would travel in the bladder, from inlet to OC exit, was about a total of 1 meter due to the internal wall (Figure 2.1b).

The OC ratio was added to the media setting of study 1-1 2D flat model. OC ratio defined the allocation of flow velocity and volume to OS and OC. It was set to 0.1, 0.25, 0.5, 0.75, 0.9 over the total outlet flow. For example, the OC ratio of 0.5 meant that the ratio of the flow velocity and volume of OC exit to OS exit was 1:1 equally, and the OC ratio of 0.25 was OC 1: OS 3.

In geometry, the 2D flat model type B was used. The feed entered from the inlet on the top left, and the cells were moved downward by the applied centrifugal force while traveling in the bladder by the flow. IN, OS, and OC were open, and the interior wall was enabled. For the media setting, the initial VF of media was 1.8×10^{-3}. The inlet flow velocity in the inlet tube was planned to be set to 0.01, 0.04, and 0.16 m/s. The number of disk

rotations controlled centrifugal force, and the range was 200, 600, and 1000 rpm. OC ratio was set to 0.1, 0.25, 0.5, 0.75, 0.9 over the total outlet flow. Each test had 10 or 30 minutes until the VF increase became a plateau. VF was measured at (1) OC exit area and (2) averaged OC area in the lower chamber.

These were the anticipated results.

- It demonstrated how the system works when used as a fully continuous operation.
- The VF of cell concentration would increase at the OC exit area if the flow effectively carried the sedimented cells without losing cells from the OS exit.
- If the flow was slow, the concentration would be high only near the inlet.

2.4 New Continuous Operation Model in Study 2

A new continuous operation model was created with COMSOL Multiphysics as an original design. The model evaluated the application of centrifugal force, gravity force, and other forces to the cells and fluid using a multiphase flow interface. The shape of the new design was a 2D symmetric model drawn as the right half of the cutaway view of the 3D model in COMSOL. The design was intended to separate cells from the supernatant and discharge both cells and supernatant simultaneously. There was no variable internal barrier. It had a separation chamber (bladder) on the outer part of the rotor. The maximum radius and height of the rotor unit and the tube diameter of inlet and outlets were the same as the Centritech type culture model in study 1. It allowed the comparison between the commercially available design and the new design.

2.4.1 Prototype Model

Figure 2.3 is the 2D prototype test model on COMSOL. The left end at r = 0 m point was the rotation center, and it was recognized as a 3D model during rotation.
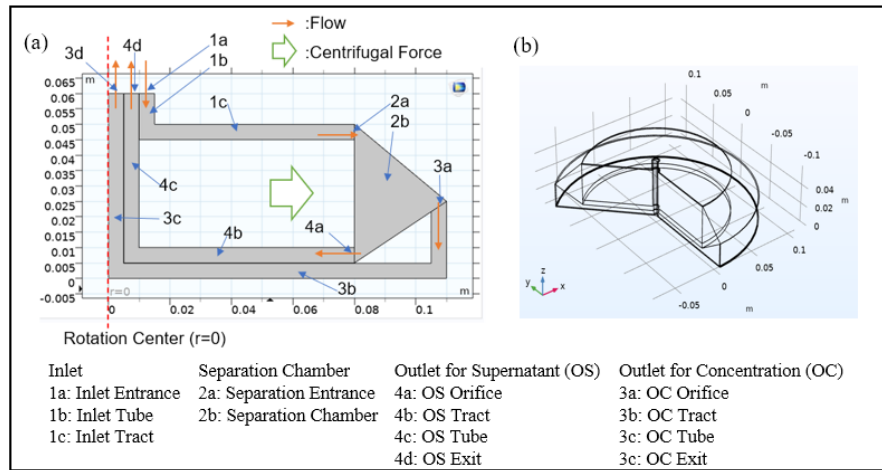
Figure 2.3 Initial design of the new continuous prototype model.
(a) prototype model drawing and name of each part, (b) 3D cutaway image.

The prototype model was made under the assumptions below, based on physical property considerations to clarify the better model structure and specification.

(1) Tubes: The tubes to this centrifuge unit were connected to the inlet tract and outlet tracts at the center of the rotation, where the centrifugal force was the lowest. Each tube had the same cross-sectional area as a default, which was the same size as the Centritech type model in study 1.

(2) Tracts: The inlet and outlet tracts were the top and bottom layers, thin disk shapes to direct the flow to the separation chamber radially and evenly. The thickness of inlet and outlet tracts affected the volumetric flow rate from and to the separation chamber. All tracts were defined as fluid transfer routes and were thinner to reduce the total fluid volume in the model.

(3) Separation chamber: The separation chamber was located at the most outer part of the model. The inside of the model was a hollow structure to take advantage of centrifuge force effectively. The separation chamber size was small enough to prevent unnecessary flow or vortexing in the chamber. The cross-sectional area of the OC orifice was the optimal size to increase the OC velocity and avoid stagnation at the OC orifice in the separation chamber by the hindered settling. Stagnation of cells might cause pelleting cells in an actual centrifuge pump.

(4) OC route: The OC orifice was located in the middle or bottom of the outer wall. The location has the highest centrifugal force. The distance from the OS tract entrance kept a certain distance, expecting to avoid the cells near OC orifice pulled into the OS route.

(5) No OC model: No OC route model (No-OC) was also made and tested.

(6) Forces: The flow direction in both OS and OC tracts opposite the centrifugal force (F_{cfg}) direction (Figure 2.4). However, the expected cell directions were different in OS and OC tracts though both were located in parallel. The cells were expected to move inward of the unit in the OC tract while moving outward in the OS tract. Fluid flow gave the cells the drag force (F_d) and virtual mass force to the same direction with the flow while pressure gradient force to the opposite direction (Harrison, 2003). If the balance between inward and outward forces in the outlet tracts was controlled, cells could theoretically move to the intended directions. The forces are explained in the appendix.
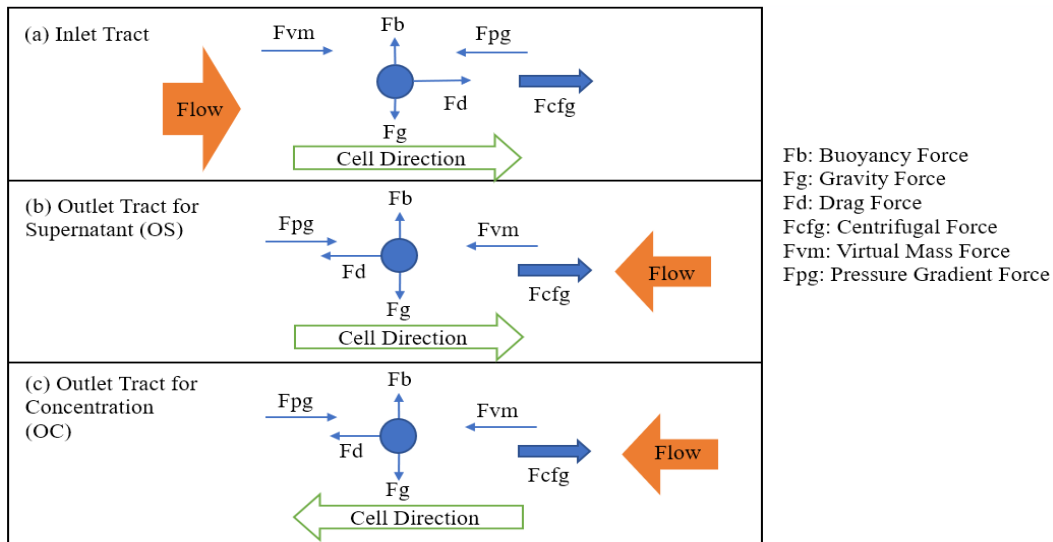
Figure 2.4 Cell direction by centrifugal force and fluid flow.
(a) inlet tract, (b) OS tract, (c) OC tract.

2.4.2 Protocol for Study 2-1

The device structure was evaluated with the new continuous operation model. The simulations ran with various media property parameters. The default test duration was 10 minutes which resulted in graphs that were not changing. Typically plateaus were reached within a few minutes of simulation, indicating steady-state operation. Structure testing included (1) inlet and outlet tract thickness, (2) separation chamber size, (3) location of the orifice to OC tract in the separation chamber, and (4) whether OC or No-OC.

Media property parameters included inlet (1) flow velocity, (2) centrifugal force (number of disk rotations), and (3) OC ratio. VF for the dispersed phase was used as an indicator of cell concentration to measure and analyze the efficiency. The initial VF of media was 1.8×10^{-3}.

2.4.2.1 Structure Test

The structure test was intended to clarify the specifications of the parts with high separation and discharge abilities. A new continuous prototype 2D symmetry model was used. Inlet tract, OS tract, OC tract thickness tested the variation of 1mm, 3mm, and 5mm thickness, respectively. The separation chamber size test changed to 5mm, 1cm, 2cm, and 3cm. OC orifice location was the entrance to the OC tract at 0cm or 2.5cm from the model's bottom. Models with and without OC tract were compared.

In the media setting, the initial VF of media was 1.8×10^{-3}. The inlet flow velocity was set to 0.16 m/s during the structure test. The number of disk rotations was 200, 600, and 1000 rpm. OC ratio was set to 0.5 fixed during the structure test. Each simulation was for 10 or 30 minutes until the VF increase became a plateau. OC model measured VF at (1) OC entrance at the edge of the rotor, (2) averaged OC tract area, and (3) OC exit located in the center of the rotor. No-OC model measured VF at only OC exit at the edge of the rotor.

These were the anticipated result.

- The set of structure tests would clarify the desirable specs for the thickness of inlet and outlet tracts, separation chamber, and OC orifice location. Otherwise, the result might be that there was no difference in changing the detailed specifications.

- For the thickness of tracts, the flow would have a higher velocity when the tracts were thinner. A thin structure was suitable for the IN tract to maintain flow velocity in the chamber and the OC tract; this carried the cells within the flowing field. On the other hand, a thick structure might be good for the OS tract, preventing the transportation of cells by counterflow.

- For the chamber size, the large chamber would have a large volume and low flow velocity, allowing for a high degree of separation. However, the centrifugal effect is weaker at the inner edge of the chamber that may cause low separation efficiency.

- For the OC orifice location, a high OC orifice would have a longer distance to the OS orifice to help avoid losing cells. On the other hand, low OC orifice might take advantage of the geometry that incoming flow from the inlet tract continues flowing along the rotor wall to the OC tract consistently.

- OC model would get lower VF at OC exit located in the center of the rotor if the flow and centrifuge balance was not matched. The No-OC model would have a higher VF concentration at the OC exit on the edge of the rotor.

2.4.2.2 Media Property Test

The media property test was intended to gather the performance data from the various structures and evaluate the relationship among the flow velocity, centrifugal force, and OC ratio. Each simulation was performed by the combination of these media property parameters.

The initial VF of media was 1.8×10^{-3}. The inlet flow velocity was set to 0.001, 0.01, 0.04, 0.08, and 0.16 m/s. The number of disk rotations was 200, 600, and 1000 rpm. OC ratio was set to 0.1, 0.25, 0.5, 0.75, 0.9 over the total outlet flow. Each test had 10 or 30 minutes until the VF increase became a plateau. OC model measured VF at (1) OC entrance at the edge of the rotor, (2) averaged OC tract area, and (3) OC exit located in the center of the rotor. No-OC model measured VF at only OC exit at the edge of the rotor.

These were the anticipated result.

- OC model and No-OC model would have different results in the cell concentration.

- The VF of dispersed cells would increase when both centrifugal force and total flow velocity rose simultaneously in the OC model. However, if the flow velocity in the OC route was not fast enough to carry the cells, the centrifugal force would be too high to decrease the VF at the OC exit.

- The No-OC model would show the correlation between the inlet flow velocity and centrifugal force positively regarding the VF of dispersed cells.

- The OC ratio parameters would affect the volume of enriched cells and the VF outcome in both the OC and No-OC models. A high OC ratio such as 0.9 needed higher centrifuge rotation to increase VF than a low OC ratio such as 0.1.

2.4.3 Protocol for Study 2-2

Study 2-2 used the model based on the structure test results of study 2-1. In addition to the parameters used in the 2-1 test, tests with additional parameters were performed to obtain extensively covered data. Additional parameters were calculated by the "$F_d = F_{cfg}$" method, the theoretical approach to balancing drag and centrifugal forces, as explained in the next section.

The model and test protocol were based on study 2-1. The initial VF of media was 1.8×10^{-3}. $F_d = F_{cfg}$ method cases used the calculated flow velocity with 200, 600, and 1000 rpm. OC ratio was set to 0.1, 0.25, 0.5, 0.75, 0.9 over the total outlet flow.

These were the anticipated results.

- $F_d = F_{cfg}$ method cases would have a better VF output than study 2-1, especially in the OC model.

- Higher parameter application cases would have higher VF if the flow and centrifuge were matched. The No-OC model would have the highest output with a higher centrifuge because collecting the cells by the OC flow was unnecessary.

In addition to the force balance by the method, two considerations were evaluated in study 2-2. The first consideration was that the VF of cells at the OC exit and OC entrance targeted the same and both high to avoid stagnation in the OC route. The second was that the VF of cells at the OS exit was minimized to remove the supernatant without losing cells.

2.4.3.1 $F_d = F_{cfg}$ Method

The flow velocity and centrifuge were calculated such that the drag force (F_d) and centrifugal force (F_{cfg}) affecting each cell were equal and balanced at the OS entrance and OC entrance. Then the flow velocity was adjusted along with the revolution speed parameters based on this "$F_d = F_{cfg}$" method (Figure 2.5). Drag force was calculated with the equation for turbulent flow. This research used the drag coefficient (C_d) given by Clift and Gauvin's equation (Clift and Gauvin, 1971).
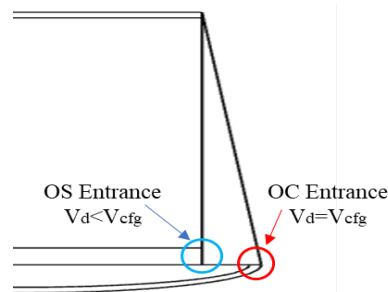
Figure 2.5 $F_d = F_{cfg}$ method in study 2-2.

The adjusted flow velocity at OS entrance was the maximum flow velocity that avoids losing cells into the OS tract, resulting in $F_d < F_{cfg}$ at this location. If the flow at the OS entrance was larger than this maximum value, the drag force would become larger than the centrifugal force in both OC and No-OC models, and the cells would flow into the OS tract.

2.4.4 Protocol for Study 2-3

This study 2-3 was a complementary consideration intended to understand the risk of shear stress in the new continuous operation model (model #1), which was made in study 2-1. The velocity of the whole route of cell concentration was evaluated in the model. There were 11 points as measuring locations: (1) inlet (IN) entrance, (2) IN tube, (3) IN tube to IN tract, (4) IN tract, (5) IN tract to separation chamber, (6) separation chamber, (7) OC entrance (separation chamber to OC tract), (8) OC tract, (9) OC tract to OC tube, (10) OC tube, and (11) OC exit. IN tube, IN tract, separation chamber, OC tract, and OC tube used averaged values in each area.

Additional models #2 and #3 were created to compare the velocity variability. Models #2 and #3 had the narrower OC entrance and the broader OS entrance at the separation chamber than model #1. Model #2 had sharp edges, and #3 had round and broad edges at the entrance of the separation chamber, the entrance of the OC tract from the separation chamber, and the entrance of the OC tube.

These were the anticipated results.

- The various cross-sectional area would change the local flow velocity.

- Additional shear stress would be brought to the cells when the flow sharply accelerated or decelerated in the centrifuge unit. The stable volume flow rate through the whole system could mitigate the shear stress leading to possible cell damage.

Chapter 3: Results

3.1 Study 1-1

The Centritech type culture model was set to a semi-continuous operation in study 1-1. The VF was measured at the OC exit and the possible discharge chamber area below the internal line. The initial volume fraction in the bladder and the fluid from the inlet was 1.8×10^{-3}, equivalent to 10^7 cells/ml. A 2D flat model type A test and a 2D symmetry model test were performed.

3.1.1 2D Flat Model (Type A) Test

During the tests, the internal wall (air barrier in the actual unit) was not used, and the whole bladder area was used as a separation area in 2D flat model type A. The OC exit was closed and wasn't used as the discharge tube.

Simulation visualized the effect of the vertical centrifugal force and the horizontal flow visually. The VF was high at the bottom, just beneath the inlet orifice when there was flow in most cases. The discharge area below the internal wall line recorded VF for the concentration of 2.3721×10^{-3}, when the inlet flow was 0.001 m/s and 600 rpm rotation.

3.1.1.1 Flow Velocity Effect in 2D Flat Model (Type A)

The effect of flow velocity on volume fraction was evaluated (Figure 3.1). Given the various flow velocity, the result showed that the lower flow velocity increased volume

fraction (VF) in this semi-continuous culture, controlling the rotation speed with 600 rpm. The average VF in the discharge area below the internal wall was 1.9638×10^{-3}, with the inlet flow velocity of 0.001 m/s in this test.
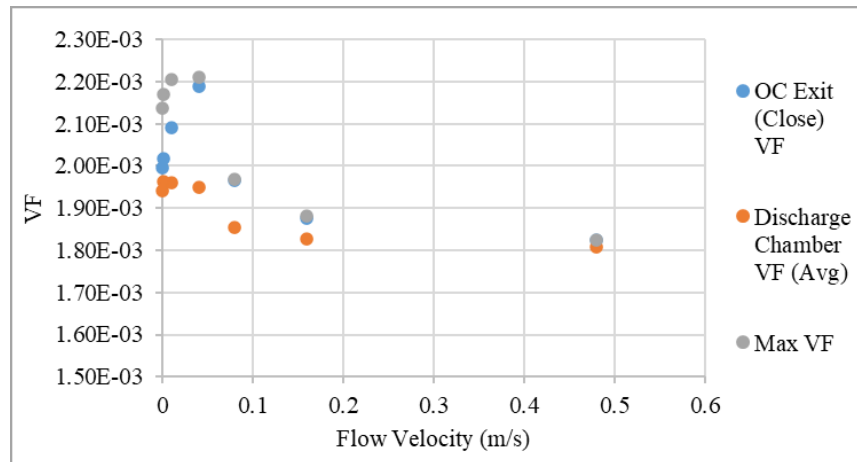
Figure 3.1 Flow velocity test in the 2D flat model (A) in study 1-1.

There were locally high VF areas, and the highest VF was 2.2095×10^{-3} with 0.04 m/s flow and 600 rpm (Figure 3.2).

3.1.1.2 Centrifugal Force Effect in 2D Flat Model (Type A)

The centrifugal force test showed that the rotation increased VF linearly, controlling the flow velocity with 0.16 m/s (Figure 3.3). Then, the rotation was increased to 2000 rpm and recorded the 2.2069×10^{-3} in the average discharge area below the internal wall line, with the 0.01 m/s flow and 2000 rpm rotation. The max VF was 2.5947×10^{-3} with a 0.01 m/s flow velocity (Figure 3.4 and 3.5).
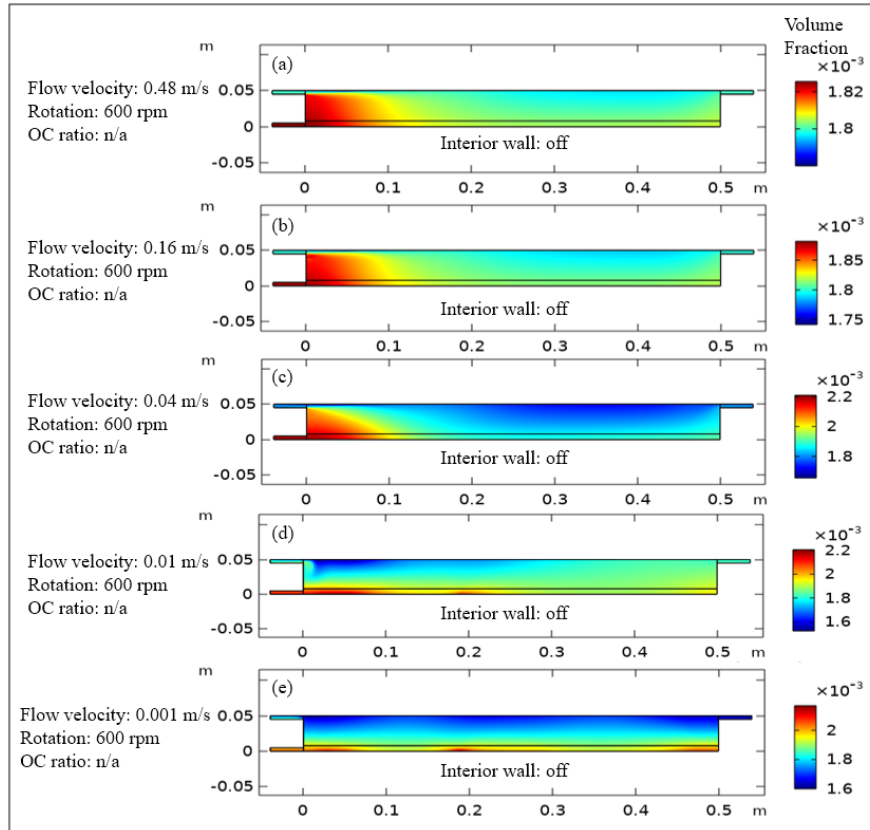
Figure 3.2 VFmap with different flow velocities in study 1-1.
(a) flow velocity 0.48 m/s, (b) 0.16 m/s, (c) 0.04 m/s, (d) 0.01 m/s, (e) 0.001 m/s in the 2D
flat model (A).
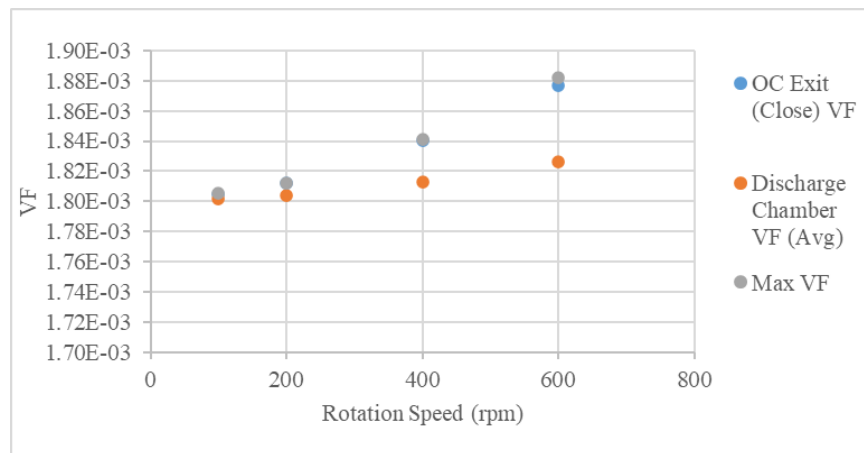
Figure 3.3 Centrifugal force test in the 2D flat model (A) in study 1-1.
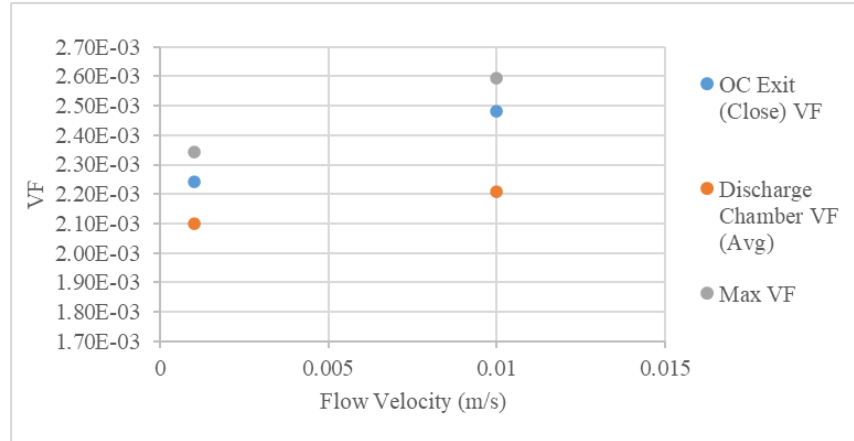
Figure 3.4 High centrifuge application in the 2D flat model (A) in study 1-1.
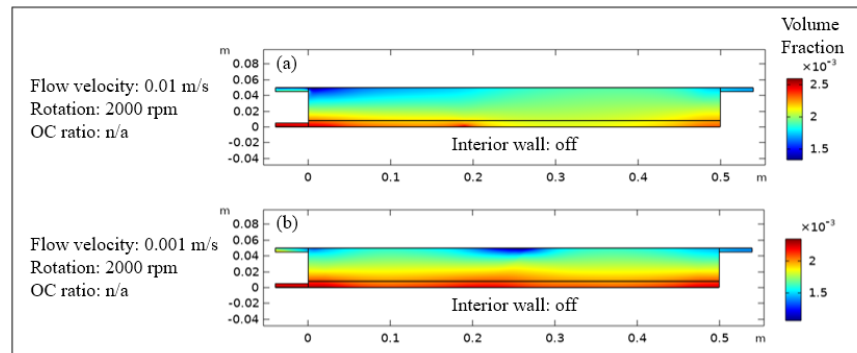
Figure 3.5 VF map with 2000 rpm in the 2D flat model (A) in study 1-1.
(a) flow velocity 0.01 m/s, (b) 0.001 m/s.

3.1.2 2D Symmetry Model Test

The 2D symmetry model test was performed to measure how much the VF of cells can be enriched in the bladder's lower area (Figure 3.6). The dispersed phase of cells, the initial VF of 1.8×10^{-3}, moved outward and downward by the applied centrifugal force.

In scenario #1, without refilling media, the VF in the lower area reached 6.3722×10^{-3} by 1000 rpm in 30 mins (Figure 3.7a). In scenario #2, with refiling of media, which kept the top of the bladder with VF 1.8×10^{-3}, the VF in the lower area reached 1.5459×10^{-2} by 1000 rpm (Figure 3.7b). When the rotation speed increased to 2000 rpm, scenario #1 reached 9.8486×10^{-3} (peak), and scenario #2 reached 2.9483×10^{-2} in 30 mins. This

result showed that Centritech Lab III has the potential to increase the cell concentration in the lower area by 3.5 times with 1000 rpm and 5.5 times with 2000 rpm even without media refilling.
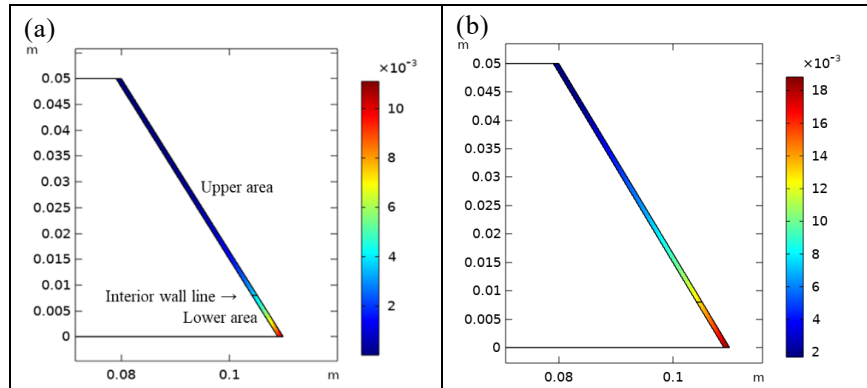
Figure 3.6 VF map in the 2D symmetry model with 1000 rpm.
(a) no refill in scenario #1, (b) continuous refill in scenario #2.
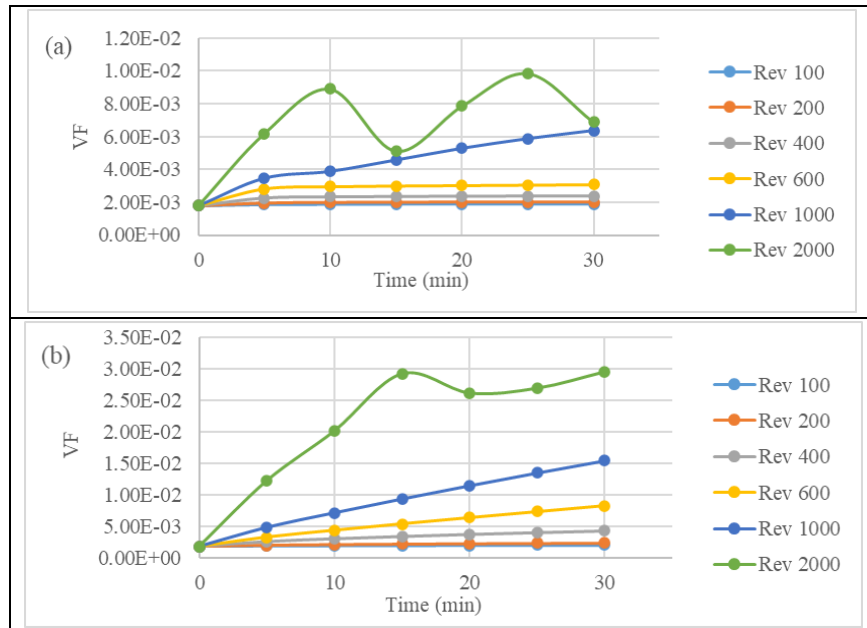
Figure 3.7 Centrifugal test in the 2D symmetry model.
(a) no refill in scenario #1, (b) continuous refill in scenario #2.

The VF in the upper area with no refill decreased to 7.8726×10^{-4} by 1000 rpm and 6.7471×10^{-4} by 2000 rpm in 30 mins in scenario #1. In scenario #2, however, continuous

refilling increased the VF in the upper area to 6.081×10^{-3} by 1000 rpm and 1.6049×10^{-2} by 2000 rpm in 30 mins. Since the media in this upper area is disposed of as supernatant from the Centritech III bladder, the low VF is desired here. This test suggested that media refilling was beneficial in cell condensation, but it might remove some cells at the same time.

Table 3.1 is a performance summary of the 2D symmetry test. This table shows that when the bladder size was 30 ml, scenario #1 with 1000 rpm could get the enriched cell fluid of 4.2 ml, of which the number of cells was 3.54×10^7/ml after 10 minutes batch process. If it had continuous refill in scenario #2 with 2000 rpm, the cells would reach 1.12×10^8/ml after 10 minutes batch process. However, this scenario #2 was artificial and not realistic, and it needed to dispose of the supernatant, including highly concentrated cells. The retrievable volume of enriched cell media (lower part) was 4.2 ml, and the supernatant was 25.2 ml per batch process.

3.2 Study 1-2

The Centritech type culture model was set to fully continuous flow condition in study 1-2. The internal wall was used during the tests, the OS exit and the OC exit were open, and the fluid was discharged continuously. The VF at the OC exit was measured with changing OC ratio.

All the tests found high VF areas near the inlet and above the interior wall in this model. Some of the flow velocity and rotation speed parameters were canceled in the set of tests because it was found out that the structure with the interior wall was not suitable for

this continuous operation. The flow velocity parameters couldn't improve the distribution of uneven cells, and rather the higher flow velocity tended to have low VF at the OC exit.

As a result, the performance in study 1-2 didn't reach the volume fraction levels in study 1-1. The inlet location might cause the sedimentation deviation, causing the fluid flow not equally in this usage. The cells might cause pellets if the system was running for a long time continuously. Therefore, the new model had a flow from the center to outward radially in study 2.

Table 3.1 Performance summary in 2D symmetry test.

Rotation (rpm), Batch time (min)	Lower Area (a) VF, (b) N of cells	Upper Area (c) VF, (d) N of cells	(e) Condensation Rate	(f) Lost Cell Rate
A, No refill in scenario #1				
1000, 10	(a) 3.8940×10^{-3} (b) 2.16×10^{7} /ml	(c) 1.3362×10^{-3} (d) 7.42×10^{6} /ml	216%	62%
1000, 30	(a) 6.3722×10^{-3} (b) 3.54×10^{7} /ml	(c) 7.873×10^{-4} (d) 4.37×10^{6} /ml	354%	37%
2000, 10	(a) 8.9022×10^{-3} (b) 4.95×10^{7} /ml	(c) 2.270×10^{-4} (d) 1.26×10^{6} /ml	495%	11%
2000, 25	(a) 9.8486×10^{-3} (b) 5.47×10^{7} /ml	(c) 1.74×10^{-5} (d) 9.66×10^{4} /ml	547%	0.8%
B, Continuous refill in scenario #2				
Rotation (rpm), Batch time (min)	Lower Area (a) VF, (b) N of cells	Upper Area (c) VF, (d) N of cells	(e) Condensation Rate	(f) Lost Cell Rate
1000, 10	(a) 7.1649×10^{-3} (b) 3.98×10^{7} /ml	(c) 3.3420×10^{-3} (d) 1.86×10^{7} /ml	398%	156%
1000, 30	(a) 1.54590×10^{-2} (b) 8.59×10^{7} /ml	(c) 6.0810×10^{-3} (d) 3.38×10^{7} /ml	859%	284%
2000, 10	(a) 2.01170×10^{-2} (b) 1.12×10^{8} /ml	(c) 7.0982×10^{-3} (d) 3.94×10^{7} /ml	1118%	331%
2000, 30	(a) 2.94830×10^{-3} (b) 1.64×10^{8} /ml	(c) 1.60490×10^{-3} (d) 8.92×10^{7} /ml	1638%	749%

3.2.1 OC Ratio Effect in Study 1-2

The OC ratio effect was evaluated, with total flow velocity 0.04, 0.16 m/s, and 200, 600 rpm rotation in initial VF 1.8×10^{-3} media. When both the OC ratio in the total flow and the flow velocity was low, the VF at the OC exit was high (Figure 3.8). Figure 3.9a shows the VF map with the OC ratio of 0.1, the flow velocity of 0.04 m/s, 600 rpm, where the highest VF at OC exit of 1.9104×10^{-3} in study 1-2. Even though the OC ratio or the flow velocity was increased or decreased, the sedimentation near the inlet couldn't change.
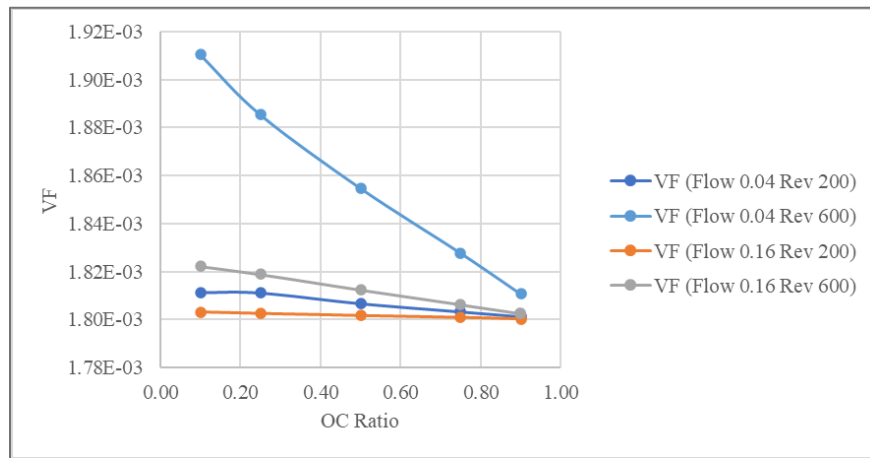
Figure 3.8 OC ratio test in the 2D flat model (B) in study 1-2.
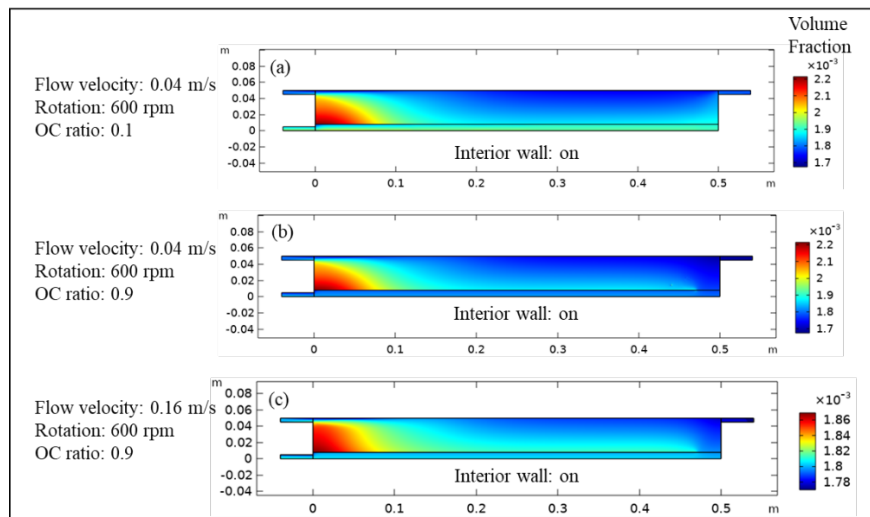
Figure 3.9 VF map in OC ratio test in study 1-2.

3.2.2 Centrifugal Force Effect in Study 1-2

Centrifugal force increased volume fraction linearly. VF at OC exit was high when the OC ratio was low, but the highest VF location was always above the interior wall. The test values were 200 and 600 rpm with the flow velocity 0.04 m/s and with different OC ratios of 0.1 to 0.9, adding 400 rpm with 0.16 m/s (Figure 3.10).
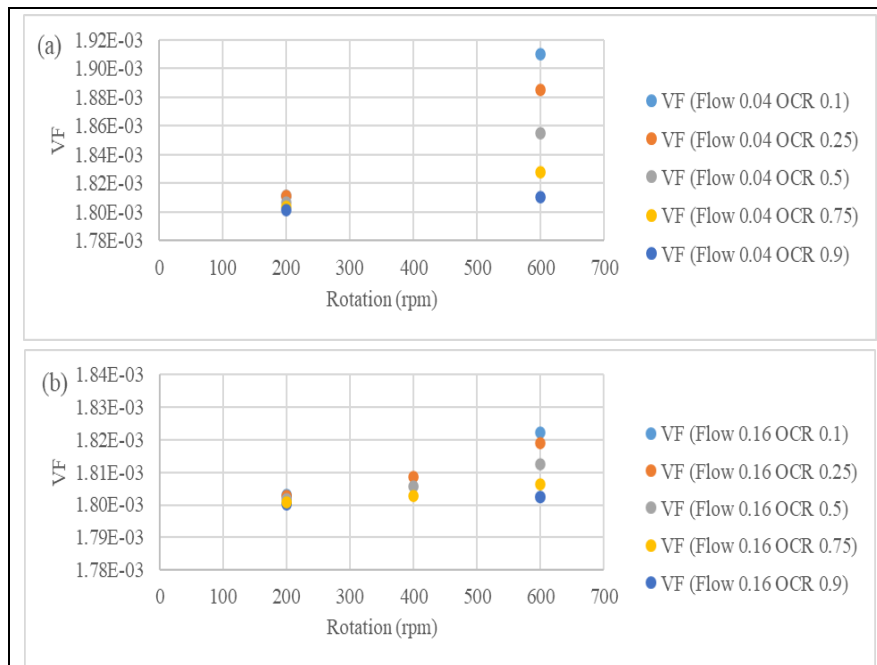
Figure 3.10 Centrifugal force test in the 2D flat model (B) in study 1-2.
(a) flow velocity 0.04 m/s, (b) flow velocity 0.16 m/s

3.3 Study 2-1

Two prototype designs of the new culture models were used in study 2-1. The OC and No-OC models were tested individually because the required physical properties differed in the OC tract and affected the specifications. Structure testing and media property testing was used to indicate the desired specifications and trends of parameter values. The initial VF of media was 1.8×10^{-3}.

3.3.1 Structure Test

Structure testing indicated the desired specifications of (1) inlet and outlet tract thickness, (2) separation chamber size, (3) location of the orifice in the OC tract of the separation chamber, both the OC and No-OC models.

3.3.1.1 OC Model Structure Test

OC model evaluated the three VF measured at OC exit, OC route average, and OC entrance. The overall evaluation selected the most desirable spec.

In the OC model thickness test, each tract thickness was tested with 1mm, 3mm, and 5mm (Figure 3.11). 1mm for the inlet and OC tracts and 3mm for OS were chosen for the OC model.

The separation chamber size was evaluated, and the smaller chamber width had a better VF for cell concentration. The chamber size of 5mm was chosen for the OC model (Figure 3.12a).

The OC orifice location was evaluated in the two different areas at the middle height (2.5cm from bottom) and the bottom (0cm from bottom). The bottom was chosen for the OC orifice for this OC model (Figure 3.12b).

As the result of the structure tests, the OC model was created (Figure 3.13). The shape of the outlet tract was modified from angular to round shape to reduce the residual cells in the angular location in the OC tract.
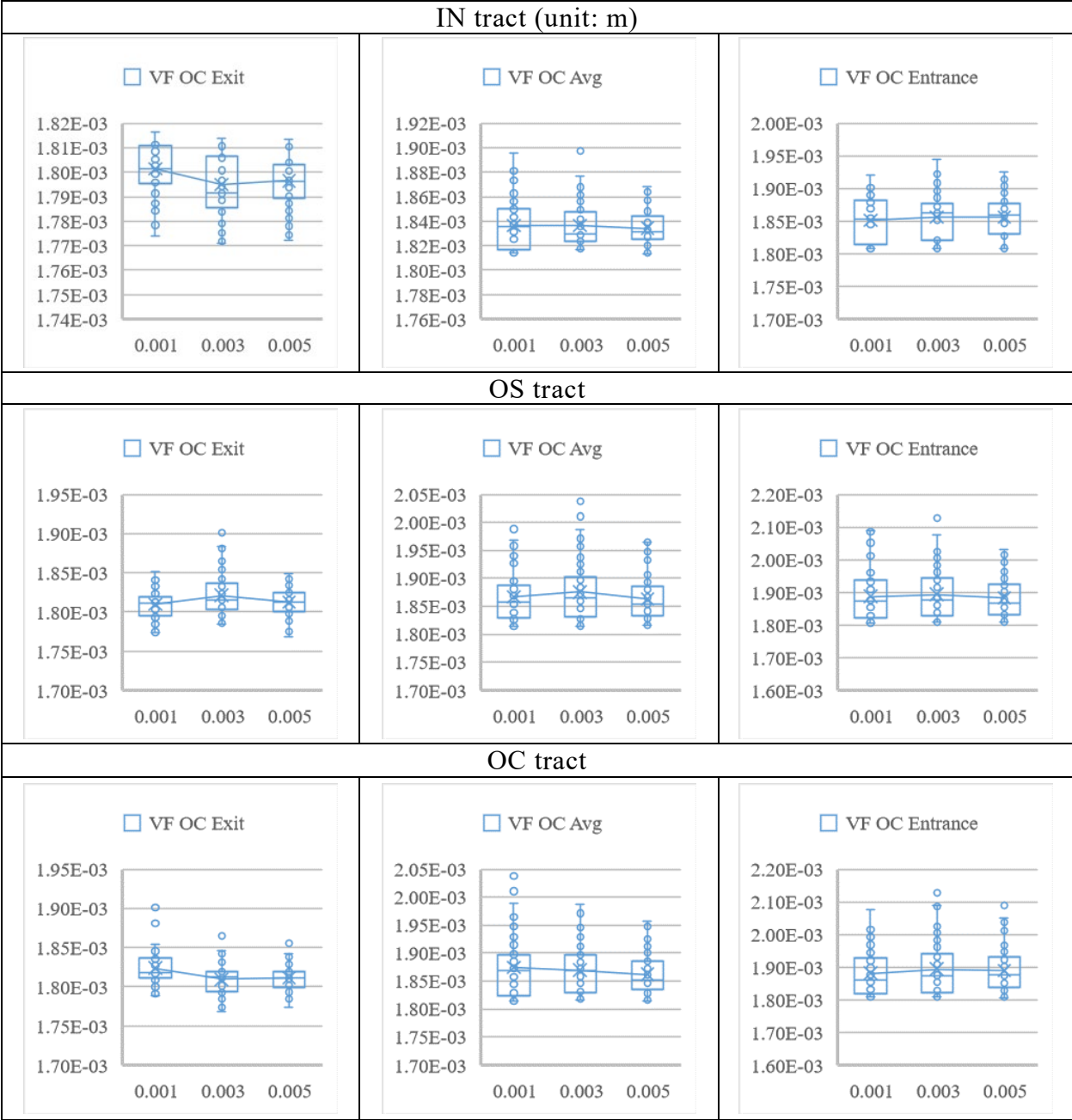
Figure 3.11 OC model thickness test.

(a) Chamber Size		
VF at OC Exit	VF at OC Average	VF at OC Entrance
(b) OC Orifice Height		
VF at OC Exit	VF at OC Average	VF at OC Entrance

Figure 3.12 OC model separation chamber size and OC orifice height test.
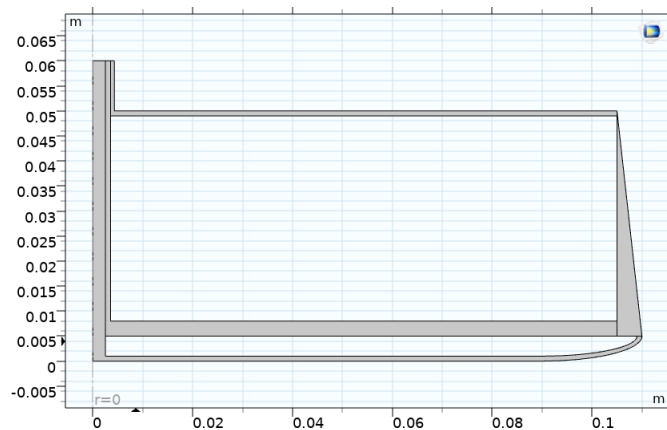
Figure 3.13 New OC model, cutaway view of right half (OC Model #1).

3.3.1.2 No-OC Model Structure Test

No-OC model evaluated the VF measurement at OC exit. The overall evaluation selected the most desirable spec. In the No-OC model thickness test, 1mm for the inlet and OC tracts and 5mm for OS were chosen for the No-OC model (Figure 3.14).

IN Tract (Unit: m)	OS Tract
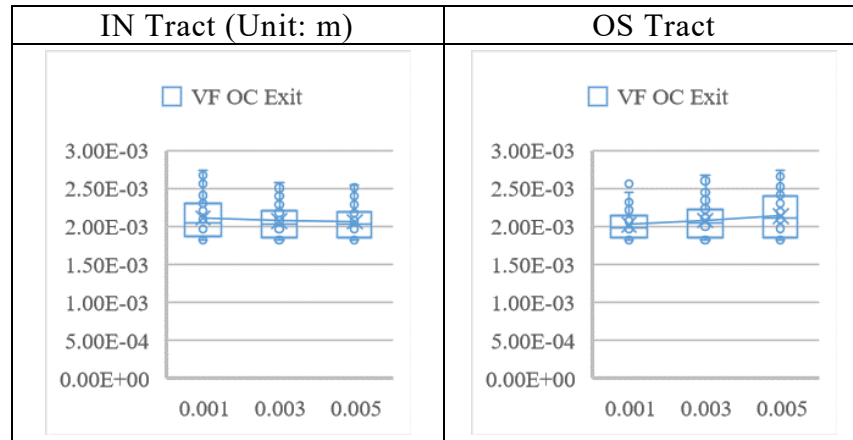
Figure 3.14 No-OC model thickness test.

The separation chamber size was evaluated, and the larger chamber had a better VF for cell concentration. A Chamber size 3cm was chosen for the No-OC model (Figure 3.15a).

The OC orifice location was evaluated in the two different areas. One was the middle height (2.5 cm from bottom), and the other was the bottom (0 cm from bottom). The bottom was chosen for the OC orifice for this OC model (Figure 3.15b).

As the result of the structure tests, the No-OC model was created (Figure 3.16). The No-OC model doesn't have an OC tract and OC tube. Concentrated cells are directly discharged from the OC exit at the bottom of the separation chamber. The test results suggested the different OS thickness and separation chamber sizes from the OC model.

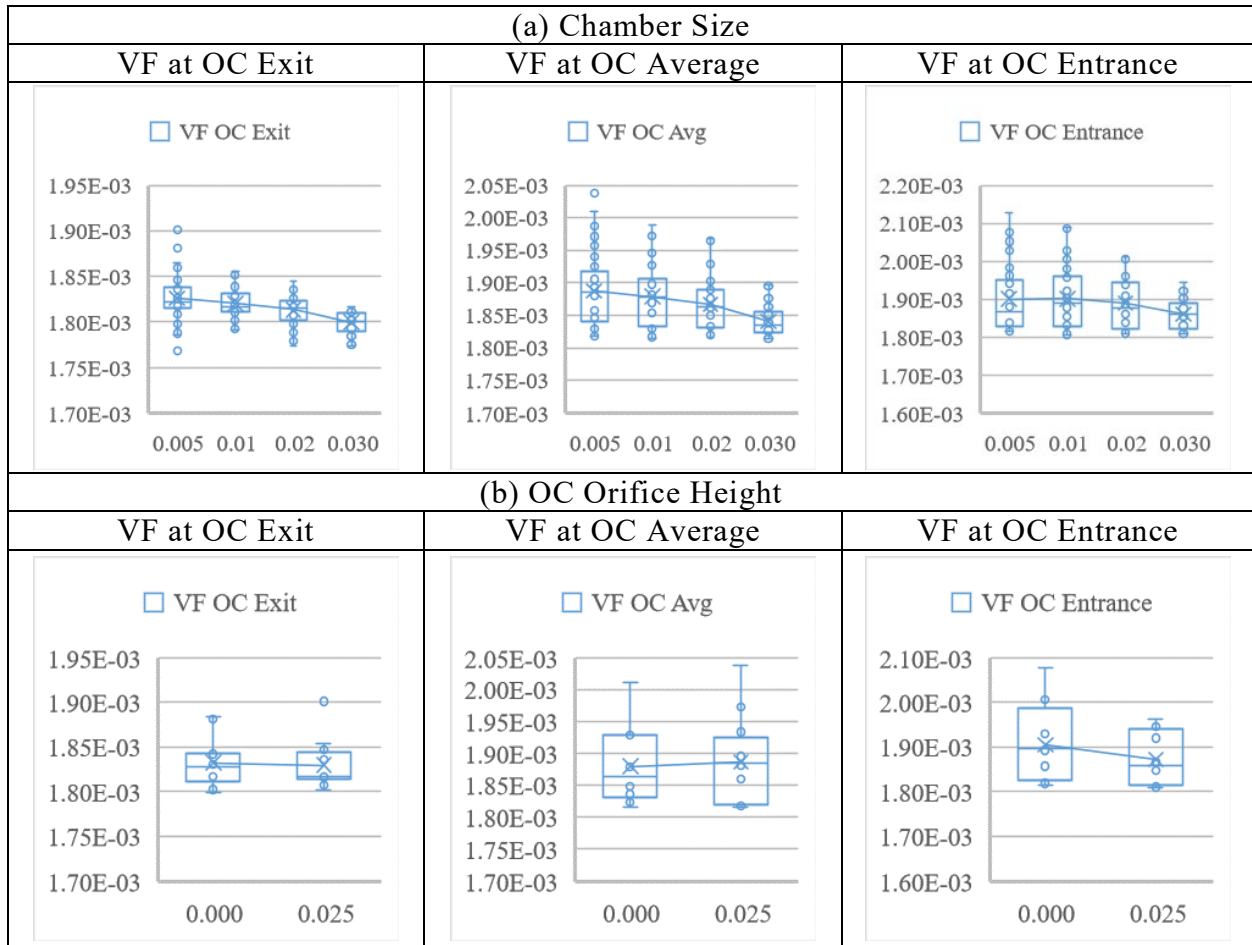| (a) Chamber Size	(b) OC Orifice Height
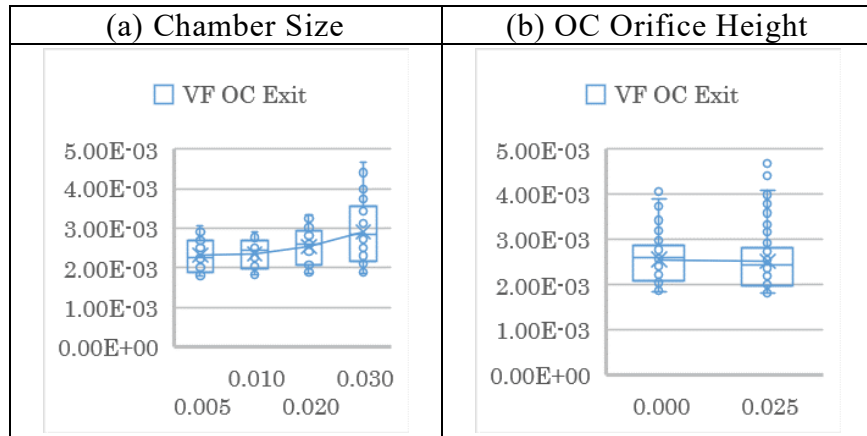
Figure 3.15 No-OC model's separation chamber size and OC orifice height test.

Figure 3.16 New No-OC model, cutaway view of right half (NoOC Model #1).

3.3.2 Media Property Test

Media parameters included inlet flow velocity, OC ratio, and the number of disk rotations for centrifugal force, using the created OC and the No-OC models.

3.3.2.1 OC Model Media Property Test

The new OC model obtained the VF measurements at OC exit, OC route average, and OC entrance. The initial VF of media was 1.8×10^{-3}. The inlet flow velocity was 0.01, 0.04, and 0.16 m/s. The number of disk rotations was 200, 600, and 1000 rpm. OC ratio was

set to 0.1, 0.25, 0.5, 0.75, 0.9 over the total outlet flow. The VF output data were recorded with changing flow velocity, revolution, and OC ratio at each location (Figure 3.17).
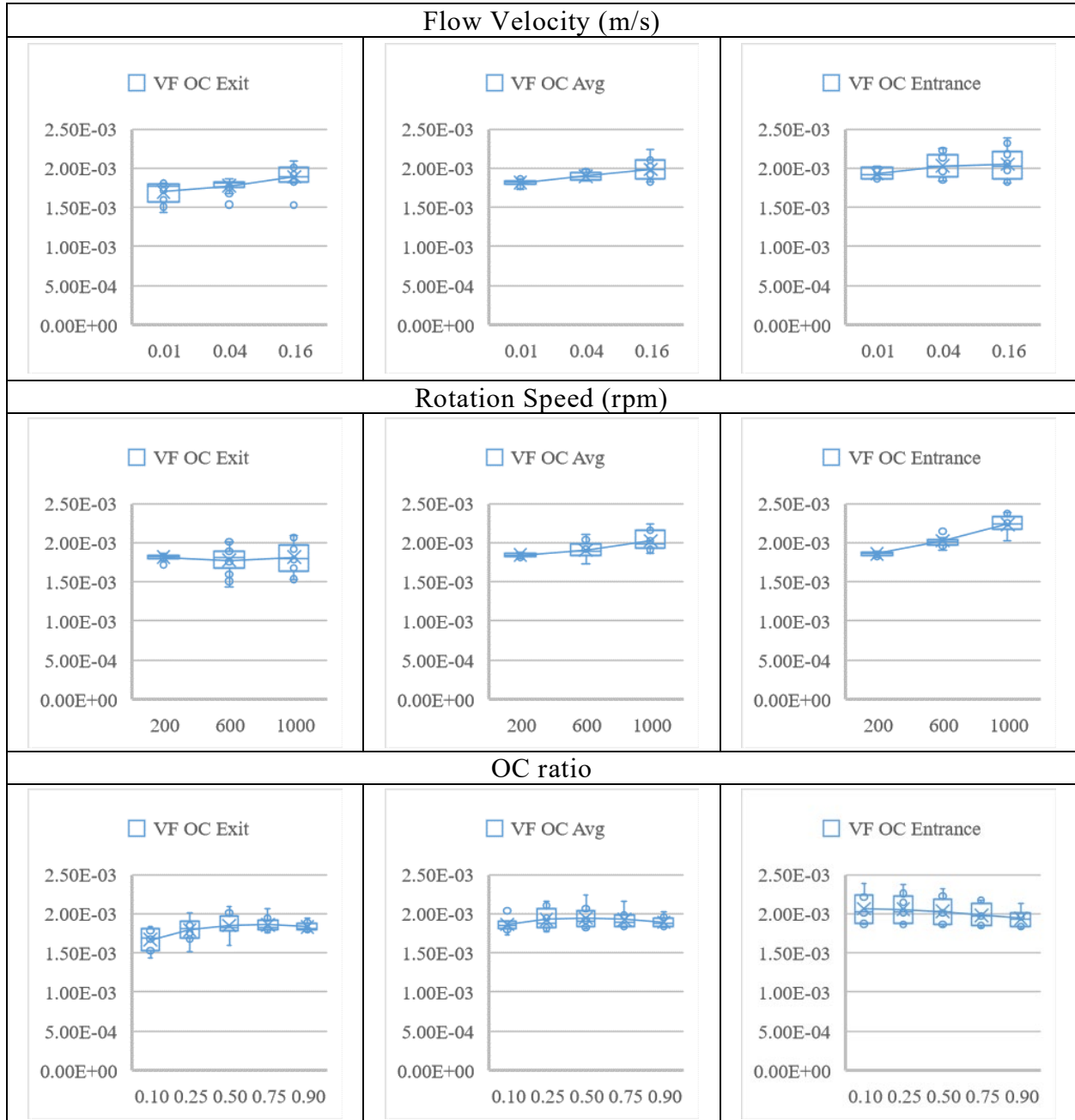
Figure 3.17 OC model media property test.

Flow velocity test showed a higher flow rate was not always good for making high VF. The Revolution test showed the higher rotations could yield high VF at the OC entrance, but it might prevent carrying the cell discharge to the OC route and the OC exit. This OC ratio test showed neither high nor low OC ratio tended to incline to either of them.

Under the limit up to 0.16 m/s and 1000 rpm, the OC model's highest VF 2.0981×10^{-3} at OC exit was obtained with a flow velocity of 0.16 m/s, OC ratio of 0.5, and rotation speed 1000 rpm (Figure 3.18). In the extensive study to increase to 2.66 m/s and 3000 rpm as maximum, the OC model reached VF 2.4068×10^{-3} at OC exit with a flow velocity of 1.5 m/s and an OC ratio of 0.5 and rotation speed 3000 rpm (Figure 3.19).
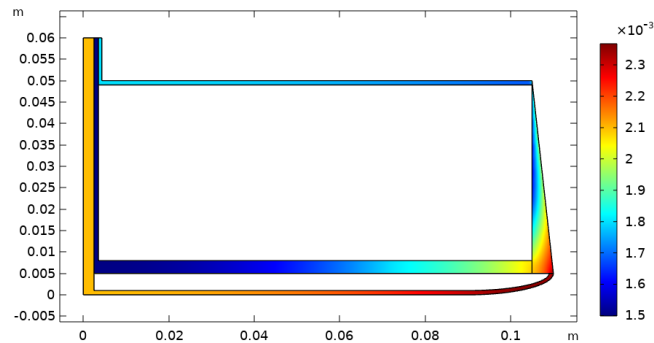
Figure 3.18 VF map of OC model at 1000 rpm.
Settings: flow 0.16 m/s, OC ratio 0.5, 1000 rpm. Results: (1) VF at OC exit 2.0981×10^{-3}, VF at OS exit 1.5008×10^{-3}, (2) condensation rate 117%, (3) lost cell rate 54%.
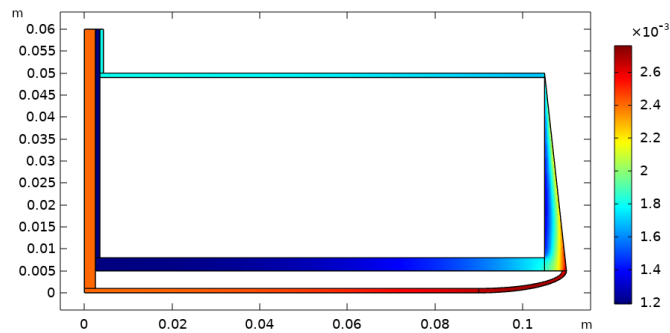
Figure 3.19 VF map of OC model with high flow and rotation speed.
Settings: flow 1.5 m/s, OC ratio 0.5, 3000 rpm. Results: (1) VF at OC exit 2.4068×10^{-3}, VF at OS exit 1.1931×10^{-3}, (2) condensation rate 134%, (3) lost cell rate 33%.

3.3.2.2 No-OC Model Media Property Test

The new OC model obtained the VF measurements at OC exit, OC route average, and OC entrance. The initial VF of media was 1.8×10^{-3}. The inlet flow velocity was set to 0.001, 0.01, 0.04, 0.08, and 0.16 m/s. The number of disk rotations was 200, 600, 1000, and 2000 rpm. OC ratio was set to 0.1, 0.25, 0.5, 0.75, 0.9 over the total outlet flow.

The VF output data were recorded with changing flow velocity, revolution, and OC ratio at OC exit (Figure 3.20).
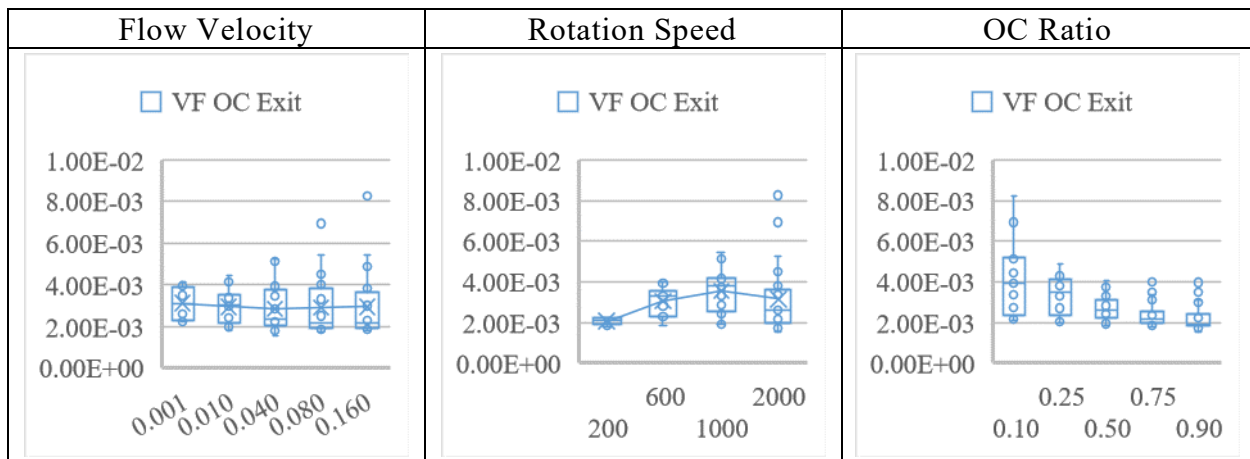
Figure 3.20 No-OC model media property test.

Flow velocity test showed a higher flow rate is not always necessary for making high VF. The Revolution test showed the higher rotations could yield high VF at the OC entrance, but when the OC ratio is high such as 0.9, the high revolution didn't work as expected. The OC ratio test showed low OC ratio could have higher condensation.

Under the limit up to 0.16 m/s and 1000 rpm, the No-OC model's highest was VF 5.4200×10^{-3} at OC exit with a flow velocity of 0.08 m/s, OC ratio of 0.1, and rotation speed 1000 rpm (Figure 3.21). When the rotation was 2000 rpm, the No-OC model's highest VF increased to 8.2504×10^{-3} with 0.16 m/s flow velocity and OC ratio 0.1 (Figure 3.22).
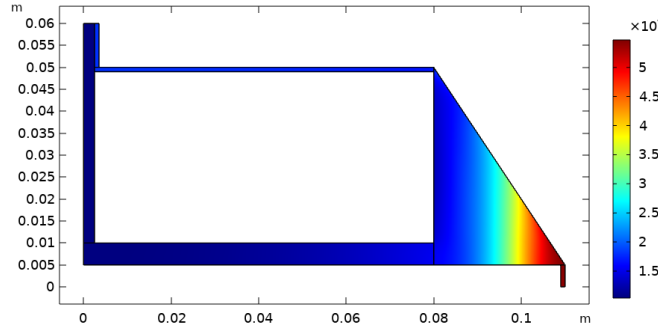
Figure 3.21 VF map of No-OC model at 1000 rpm.
Settings: flow 0.08 m/s, OC ratio 0.1, 1000 rpm. Results: (1) VF at OC exit 5.4200×10^{-3}, VF at OS exit 1.0383×10^{-3}, (2) condensation rate 301%, (3) lost cell rate 52%.
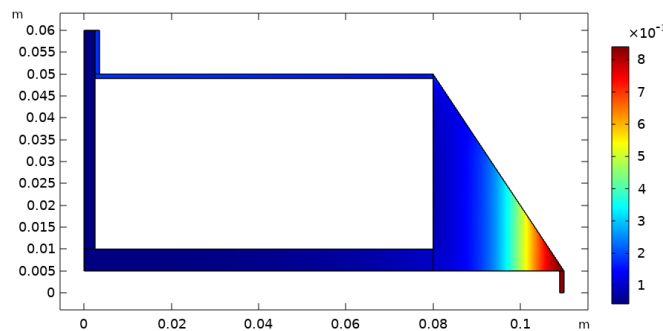

Figure 3.22 VF map of No-OC model at 2000 rpm.
Settings: flow 0.16 m/s, OC ratio 0.1, 2000 rpm. Results: (1) VF at OC exit 8.2504×10^{-3}, VF at OS exit 4.3410×10^{-4}, (2) condensation rate 458%, (3) lost cell rate 22%.

3.4 Study 2-2

Additional parameters were calculated by the $F_d = F_{cfg}$ method. The set of the simulation was performed in OC model #1. Also, the setting for supernatant removal was assessed, minimizing the lost cell rate.

3.4.1 $F_d = F_{cfg}$ Method

The adjusted flow velocity values were calculated along with revolutions 200, 600, and 1000 rpm to start the simulation. The balanced locations were (1) OC entrance and (2) OS entrance, where the length from the rotor center was 11cm and 10.5cm, respectively.

The OC entrance was the minimum required flow point that moves cells inward through the OC tract when $F_d > F_{cfg}$. The OS entrance was the maximum flow limit point that prevented cells from entering the OS tract when $F_d < F_{cfg}$. Figure 3.23 shows the relationship between the minimum required flow velocity at the OC entrance and the maximum flow limit at the OS entrance. The OC ratio varied the applied flow velocities.
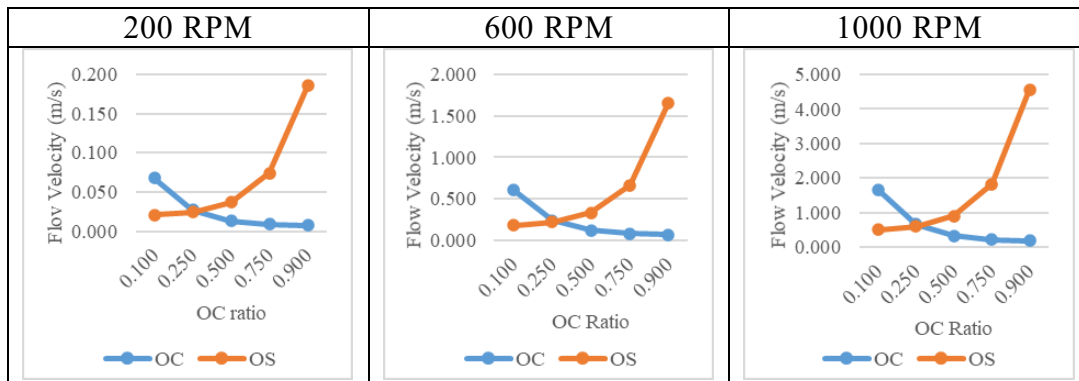
Figure 3.23 Flow velocity based on $F_d = F_{cfg}$ method.

Figure 3.24 is the simulation result when both the minimum required and maximum limit flow velocities were given to the flow parameter on the simulations. Figure 3.24a is the distribution of VF per applied flow velocity, and figure 3.24b is the VF by OC ratio. When the rotation speed was 1000 rpm, adjusting the flow velocity with the minimum required flow velocity at OC yielded higher VF than adjusting to the maximum limit flow velocity at OS in 4 of 5 OC ratio categories. But, the trends looked differently in each rotation speed, though the flow velocity parameters were given by the same equation.

When the force balance at OC entrance was adjusted to $F_d = F_{cfg}$, the highest VF at OC exit was 2.2066×10^{-3} and increased 23%, having set to OC ratio 0.25 and 1000 rpm with the adjusted flow velocity of 0.667 m/s. The VF at the OC entrance was 2.2693×10^{-3}, and the VF difference between the OC exit and entrance was 6.27×10^{-5} as 3%. The cells

were discharged with supernatant, and the lost cell rate was 69% because the OC ratio setting was 0.25, allocating 75% of fluid to OS (Figure 3.25).
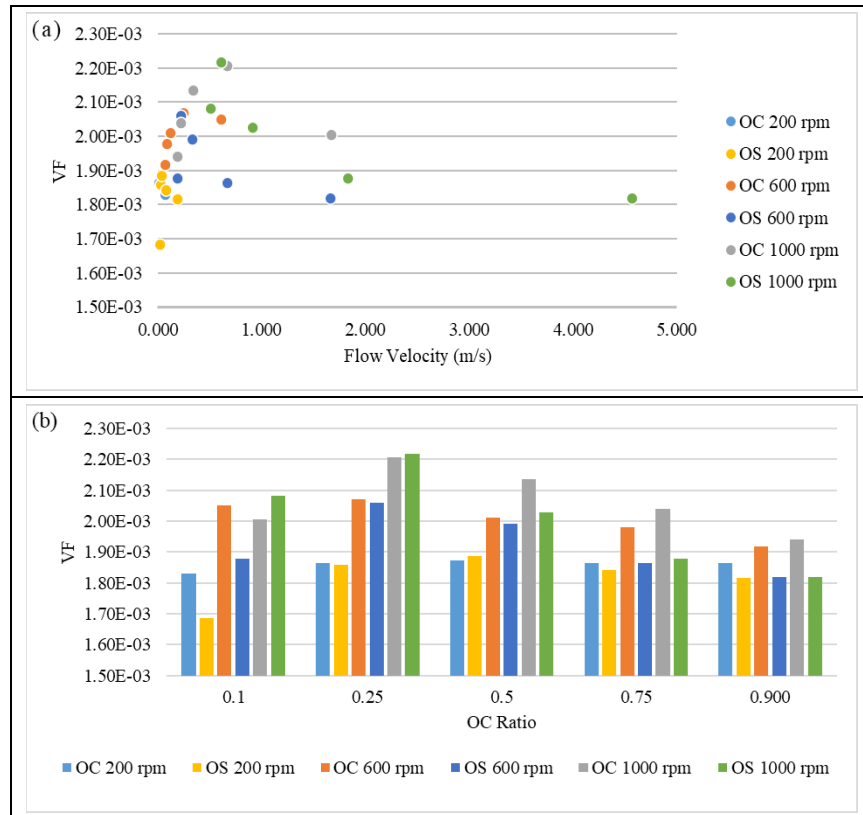
Figure 3.24 VF at OC exit based on $F_d = F_{cfg}$ method.
(a) VF distribution by flow velocity, (b) VF distribution by OC ratio.
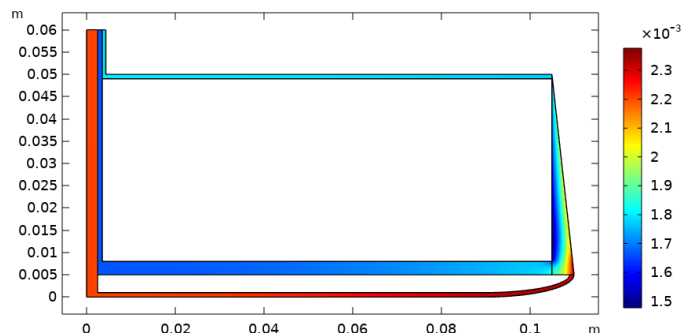
Figure 3.25 VF map of OC model with the adjusted flow velocity by $F_d = F_{cfg}$ method. Settings: flow 0.667 m/s, OC ratio 0.25, 1000 rpm. Results: (1) VF at OC exit 2.2066×10^{-3}, VF at OS exit 1.6645×10^{-3}, (2) condensation rate 123%, (3) lost cell rate 69%.

3.4.2 Statistical Approach

For the performance assessment, correlation with media property variables was calculated in the OC model tests, including extensive parameters up to flow velocity 2.657 m/s and 3000 rpm. Correlation analysis indicated that the inlet flow velocity and rotation speed correlate, but the OC ratio doesn't correlate with flow velocity or rotation (Table 3.2).

Table 3.2 Correlation in media property variables (Pearson).

(N=165)	VF OC Exit	VF OC Avg	VF OC Entrance	Inlet Flow	OC Ratio	Rotation Speed
VF OC Exit	1	.594**	-.247**	.454**	0.13	.173*
VF OC Avg	.594**	1	.620**	.399**	-.162*	.833**
VF OC Entrance	-.247**	.620**	1	0.058	-.297**	.821**
Inlet Flow Velocity	.454**	.399**	0.058	1	0.05	.427**
OC Ratio	0.13	-.162*	-.297**	0.05	1	-0.127
Rotation Speed	.173*	.833**	.821**	.427**	-0.127	1

** Correlation is significant at the 0.01 level (2-tailed).
* Correlation is significant at the 0.05 level (2-tailed).

The analysis of standardized coefficient beta indicated that the flow velocity positively affected the VF at OC exit at the rotor center (Table 3.3). It suggested that the flow in the OC tract had a critical role in carrying cells to the rotor center, and a certain amount of high flow rate was necessary to have high rate retention at the discharge stage. On the other hand, it negatively affected the VF at the OC entrance on the rotor edge as the faster the flow, the lower the VF in the separation stage at the OC entrance. It suggested the fast flow prevented the high rate separation, and the slow flow was desired in the separation stage. The rotation speed significantly affected the VF at the OC entrance, so a higher rotation speed was essential for successful cell separation.

Table 3.3 Linear regression in media property variables.

Model	Variables	Standardized Coefficients Beta	t	Significance
VF at OC Exit (Center or the Rotor)	(Constant)	-	56.905	<.001[*]
	Inlet Flow Velocity	.451	6.167	<.001[*]
	Out2c Flow Ratio	.107	1.596	.112
	Rotation Speed	-.006	-0.088	.93
VF at OC Entrance (Edge of the Rotor)	(Constant)	-	72.367	<.001[*]
	Inlet Flow Velocity	-.337	-9.181	<.001[*]
	Out2c Flow Ratio	-.160	-4.791	<.001[*]
	Rotation Speed	.944	25.557	<.001[*]

[*] -- $p < 0.05$

These results showed that it was better to set the flow to the minimum flow to collect the cells into the OC tract and use a high rotation speed. When moving the cells inward at the rotor edge where the centrifugal force was the strongest, it was considered that this location should be the force balance point of $F_d = F_{cfg}$ for the cells.

3.4.3 Consideration of Supernatant Removal

Although some models got higher VF with a high condensation rate, the lost cell rate was not always low, especially in the OC models. This section focused on the supernatant removal and assessed the lower lost cell rate cases in the OC. The cases were limited to the OC ratio of 0.9. It means that OC exit has 90% of the flow volume goes to OC exit, and 10 % goes to OS exit. If the device can't suppress cell outflow, simply 10% of cells go away from the device as supernatant. When centrifugation can retain the cells, and the flow carries all or almost all of the cells into the OC route, the supernatant doesn't include the cells, resulting in low VF at OS exit and a low lost cell rate.

The collected data up to the flow velocity 1.0 m/s were plotted to seek the lowest VF at OS exit and identify with 200, 600, 1000, and 2000 rpm rotation speed (Figure 3.26).

The faster the rotation speed, the lower the VF at OS exit, resulting in a low lost cell rate. However, as the OS value approached the minimum, the difference between OC exit and OC entrance increased, causing possible stagnation of the cells at the OC entrance.

The data of minimum required flow velocity by the $F_d = F_{cfg}$ method was compared with other data points. The rectangles in Figure 3.26 are VF results with the minimum required flow velocity of the $F_d = F_{cfg}$ method. The difference between the OC exit and OC entrance was low as expected at 1000 and 2000 rpm. However, it didn't have the lowest VF at OS exit at all speeds.
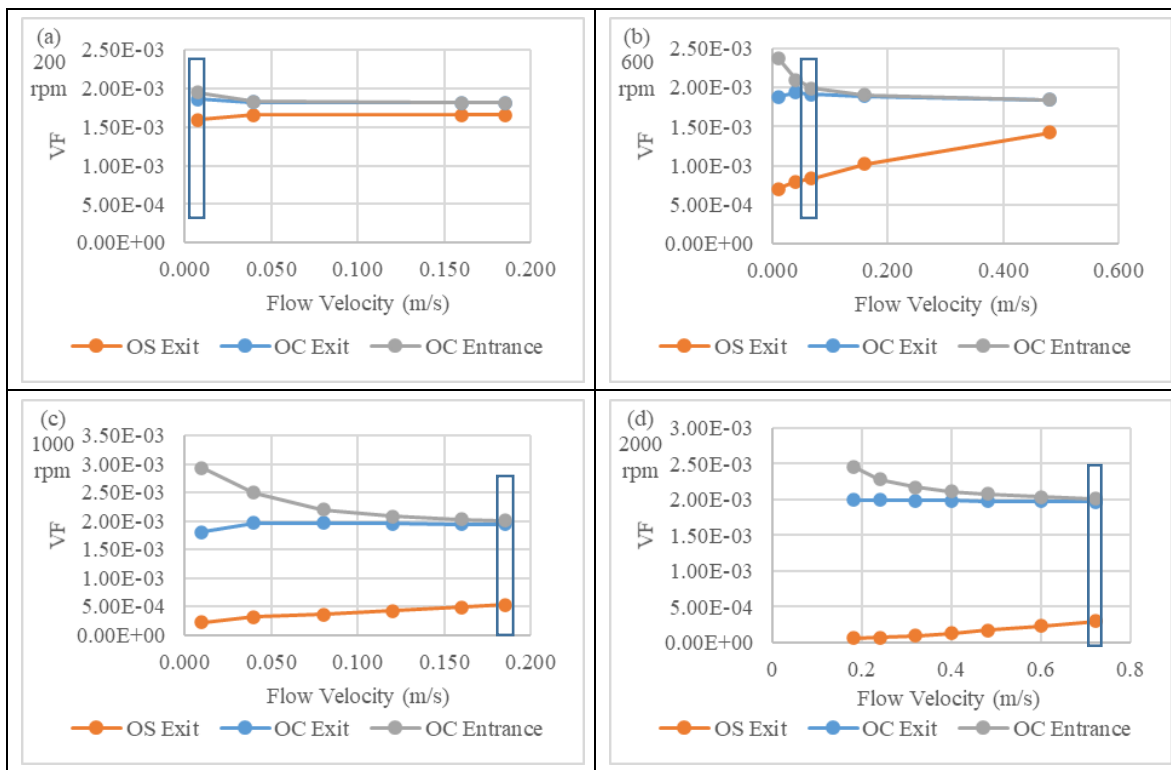
Figure 3.26 Relationship among OS exit, OC exit, and OC entrance.
The rectangles are the minimum required flow velocity adjusted by the $F_d = F_{cfg}$ method.

When the flow velocity came to lower, VF at the OS exit became lower at all rotation speed. There was a difference of the lowest level of VF by the given rotation speed.

For example, in the OC model cases of the rotation speed of 1000 rpm, when the flow velocity was 0.08 m/s, and the OC ratio was 0.9, VF at OS exit was 3.648×10^{-4}, and the lost cell rate was 2% (Figure 3.27). In the rotation of 2000 rpm, when the flow velocity was 0.32 m/s, and the OC ratio was 0.9, VF at OS exit was 9.82×10^{-5}, and the lost cell rate was 0.5% (Figure 3.28). Both cases increased only 9% and 11% of condensation rate, but they showed the possibility of continuous media replacement without losing many cells.

Figure 3.27 VF map of OC model for supernatant removal at 1000 rpm.
Settings: flow 0.08 m/s, OC ratio 0.9, 1000 rpm. Results: (1) VF at OC exit 1.9652×10^{-3}, VF at OS exit 3.648×10^{-4}, (2) condensation rate 109%, (3) lost cell rate 2.0%.

Figure 3.28 VF map of OC model for supernatant removal at 2000 rpm.
Settings: flow 0.32 m/s, OC ratio 0.9, 2000 rpm. Results: (1) VF at OC exit 1.9891×10^{-3}, VF at OS exit 9.82×10^{-5}, (2) condensation rate 111%, (3) lost cell rate 0.5%.

Table 3.4 is the summary of these two cases. Since these devices are continuously operating, the volumetric flow of concentration and supernatant can be accumulated. In the first case with 1000 rpm, 94 ml of supernatant was discharged with disposing of 2% of cells

54

in 10 minutes. In the second case with 2000 rpm, 377 ml of supernatant was removed with disposing of 0.5% of cells in 10 minutes. Since the OC model's inner volume is approximately 384 cm^3, these two cases actively removed the supernatant. The active media exchange had the potential to give a fresh and nutritious condition to the retained cells.

Table 3.4 Performance summary in OC model for supernatant removal.

OC Model					
Rotation, Velocity, OC ratio	OC Exit (a) VF, (b) N of cells	OS Exit (c) VF, (d) N of cells	(e) Condensation Rate	(f) Lost Cell Rate	Removed supernatant volume (g) Volumic flow rate, (h) Accumulated in 10 mins
1000 rpm, 0.08 m/s, 0.9	(a) 1.9652×10^{-3} (b) 1.097×10^7 /ml	(c) 3.648×10^{-4} (d) 2.03×10^6 /ml	109%	2%	(g) 0.16 ml/s (h) 94.2 ml
2000 rpm, 0.32 m/s, 0.9	(a) 1.9891×10^{-3} (b) 1.11×10^7 /ml	(c) 9.82×10^{-5} (d) 5.46×10^5 /ml	111%	0.5%	(g) 0.63 ml/s (h) 377.0 ml

As an additional consideration, supernatant removal cases were assessed in some No-OC cases. In the No-OC model cases of the rotation speed of 1000 rpm, when the flow velocity of 0.01 m/s and the OC ratio of 0.9, VF at OS exit was 1.701×10^{-4}, the lost cell rate was 0.9%, and the removable supernatant in 10 minutes was 11.8 ml (Figure 3.29). When the flow velocity increased to 0.08 m/s, VF at OS exit was 2.332×10^{-4}, the lost cell rate was 1.3%, and the removable supernatant in 10 minutes was 94.2 ml. In the higher rotation of 2000 rpm, when the flow velocity of 0.01 m/s and the OC ratio of 0.9, VF at OS exit was 3.2×10^{-6}, and the lost cell rate was 0.02%. However, the flow was too slow to

supply enough cells to the separation chamber, resulting in the low VF at the OC exit after

10 mins. (Figure 3.30).

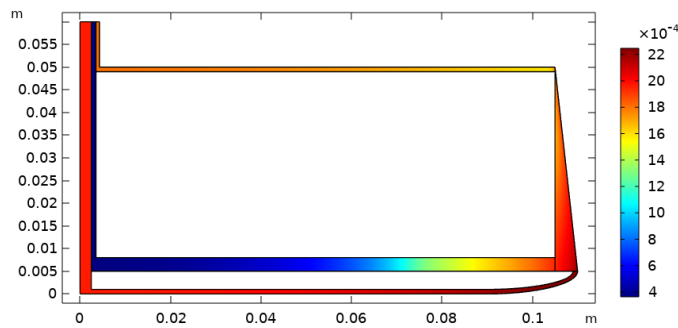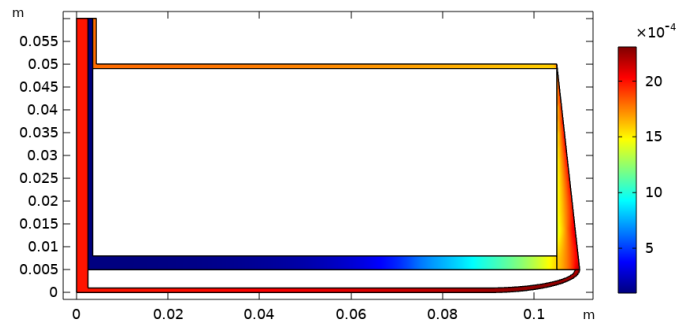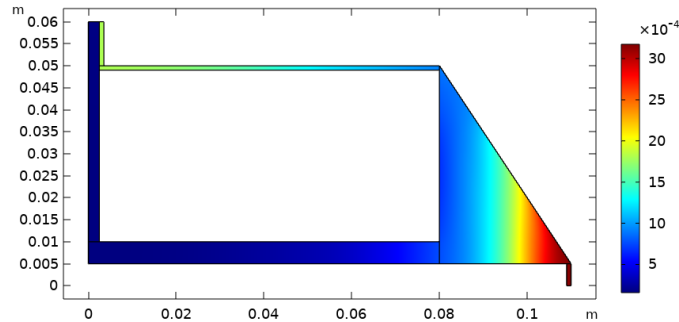
Figure 3.29 VF map of No-OC model for supernatant removal at 1000 rpm.
Settings: flow 0.01 m/s, OC ratio 0.9, 1000 rpm. Results: (1) VF at OC exit 3.1440×10^{-3},
VF at OS exit 1.701×10^{-4}, (2) condensation rate 175%, (3) lost cell rate 0.9%.
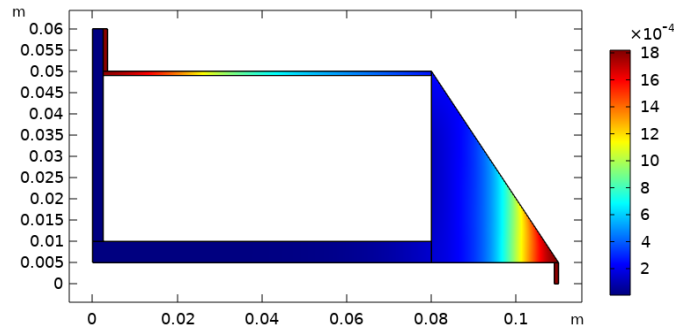
Figure 3.30 VF map of No-OC model for supernatant removal at 2000 rpm.
Settings: flow 0.01 m/s, OC ratio 0.9, 2000 rpm. Results: (1) VF at OC exit 1.7870×10^{-3},
VF at OS exit 3.2×10^{-6}, (2) condensation rate 99%, (3) lost cell rate 0.02%.

3.4.4 Comparison of Models

Table 3.5 is a comparison chart for Centritech Lab III type models for semi-continuous and continuous use and new OC and No-OC models. Centritech model for semi-continuous use had high cell concentration at exit stream; however, the batch-wise operation limited the volume of cell concentration to 4 to 5 ml and removable supernatant to about 20 to 25 ml per batch. Centritech model for continuous use had the lowest cell concentration at exit stream and had possible cell stagnation by sedimentation on the internal or bottom

walls or settling cells near the inlet by centrifugal force. The OC model could manage the cell stagnation possibility and lost cells by adjusting the flow velocity, removing supernatant without losing many cells. The No-OC model had high cell concentration in the exit stream and could remove the supernatant without losing many cells. However, the No-OC model needs an additional cell collection device or method for a clean environment operation or a closed system to prevent contamination.

Table 3.5 Comparison of Centritech type and new models.

	Centritech (Semi-continuous)	Centritech (Continuous use)	New model OC model	New model No-OC model
Operation manner	Batch-wise	Fully continuous	Fully continuous	Fully continuous
Cell concentration at exit stream	High, but 4-5 ml per batch	Very low[*]	Not high as Centritech semi-continuous and No-OC	High
Cell stagnation possibility	Low (slow flow), High (fast flow)	High[*]	Manageable (need adjustment)	Low
Lost cells in the supernatant	Low (slow flow), High (fast flow)	Low (slow flow), High (fast flow)	Manageable (need adjustment)	Low
Removable supernatant volume	Low[*], 20-25 ml per batch	Depending on the flow volume	Depending on the flow volume	Depending on the flow volume
An additional cell collection device	No	No	No	Yes[*]

[*] Critical problem and limitation.

3.5 Study 2-3

The flow velocity and stability in the cell's flow routes were analyzed with three models to assess the possible factors for shear stress, including the new model of study 2-2.

3.5.1 New OC Model #2 and #3 Based on Velocity Consideration

New OC models #2 and #3 were created for velocity consideration (Figure 3.31 and 3.32). Since the local flow velocity was considered to be affected by the cross-sectional area at the outlet orifices from the separation chamber, these new models #2 and #3 had the narrower OC entrance and the broader OS entrance at the separation chamber. The new model #2 had sharp edges, and #3 had round and broad edges at the entrance of the separation chamber, the entrance of the OC tract from the separation chamber, and the entrance of the OC tube. The VF for cell concentration of the new model #2 was 1.9735×10^{-3}, and #3 was 1.8623×10^{-3} at the OC exit.
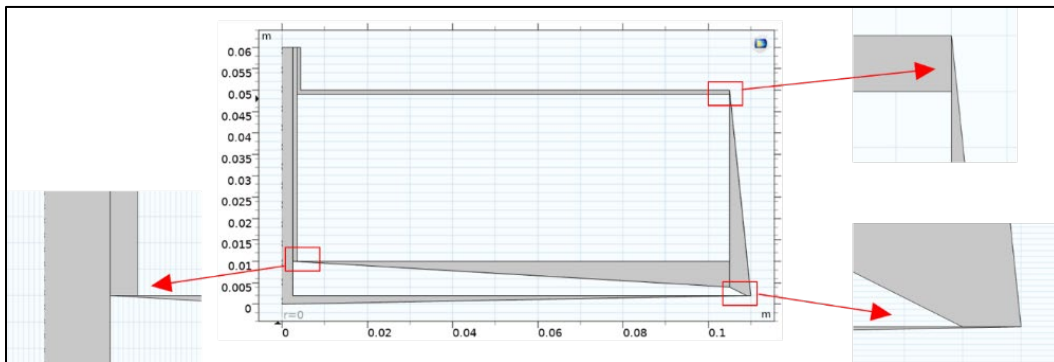
Figure 3.31 New OC model #2 with sharp edges.
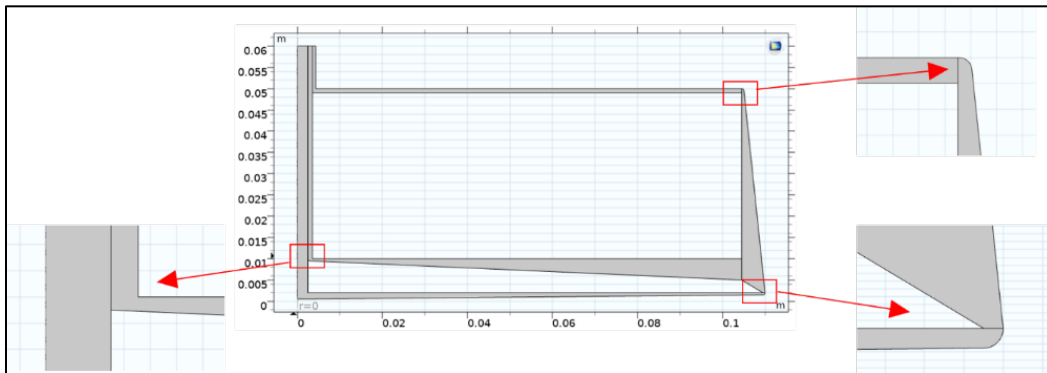
Figure 3.32 New OC model #3 with round and broad edges.

3.5.2 Velocity Analysis

The velocity of the whole route of cell concentration was evaluated in the new models. Figure 3.33 shows the velocity magnitude of the three models. Eleven points were used as measuring locations: IN entrance, IN tube, IN tube to IN tract, IN tract, IN tract to a separation chamber, separation chamber, OC entrance (separation chamber to OC tract), OC tract, OC tract to OC tube, OC tube, and OC exit. Velocity at the tubes, tracts, and separation chamber was average in the areas. Velocity slowed down in the inlet tract and got back at the OC tube.
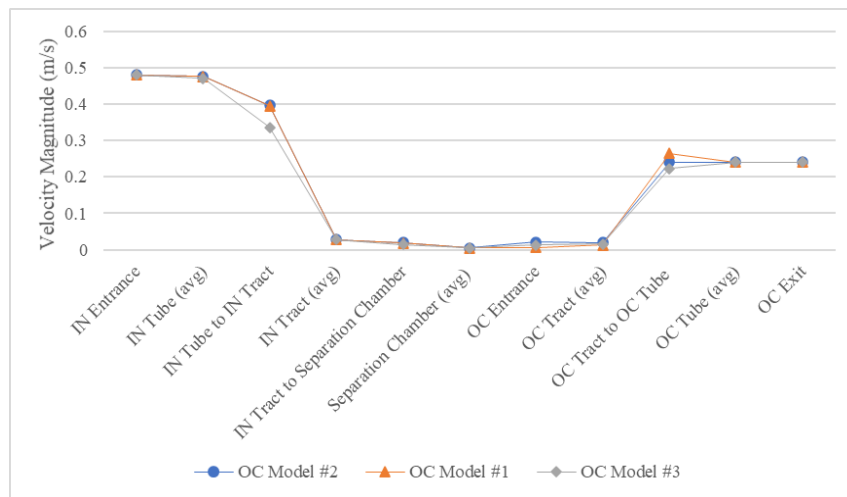
Figure 3.33 Velocity magnitude analysis in study 2-3.

The velocity magnitude map in each model shows the detail. The local fast velocity areas were found in narrow spaces. OC model #1 had one acceleration spot at the narrow entrance to the separation chamber (Figure 3.34). Model #2 had two acceleration spots at the narrow entrances to the separation chamber and the OC entrance (Figure 3.35). Although model #3 was similar to model #2, the local flow velocity was not as fast as #2 (Figure 3.36).

It was considered that the narrow area of the OC orifice in model #2 worked like a pump explained by Pascal's principle, increasing the local flow velocity and the force to help the cells to move out from the separation chamber.
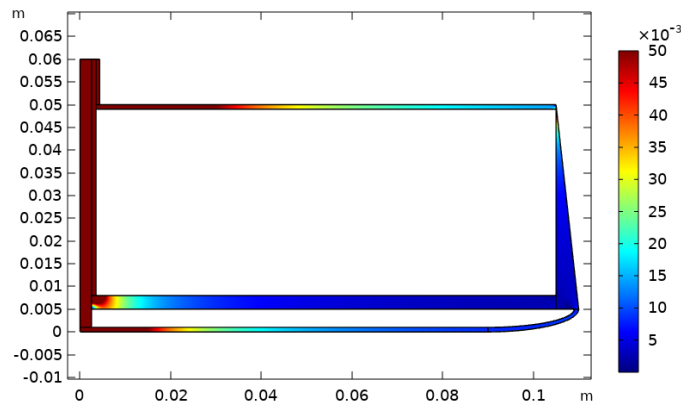
Figure 3.34 Velocity map of OC model #1 (unit: m/s).
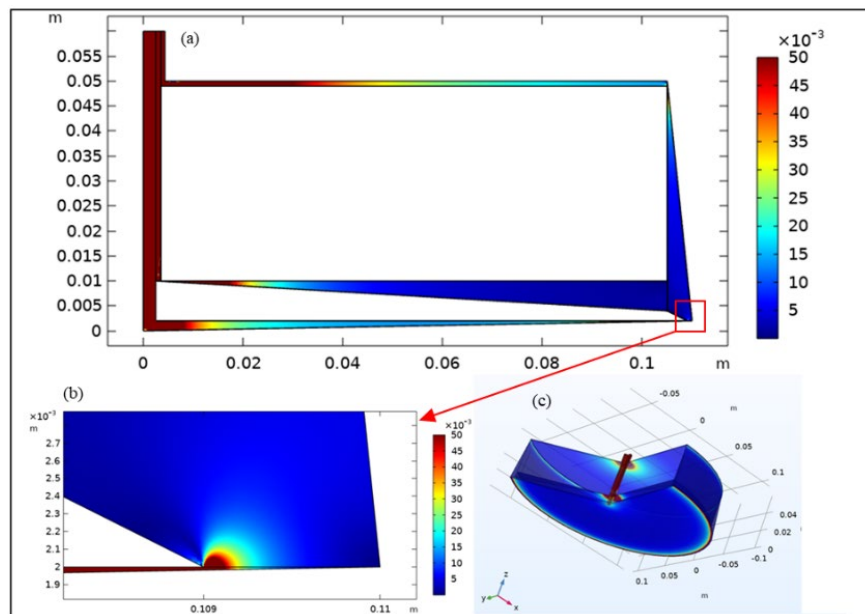
Figure 3.35 Velocity map of OC model #2 (unit: m/s).
(a) velocity map, (b) the narrow OC entrance from the separation chamber, (c) view from the bottom.
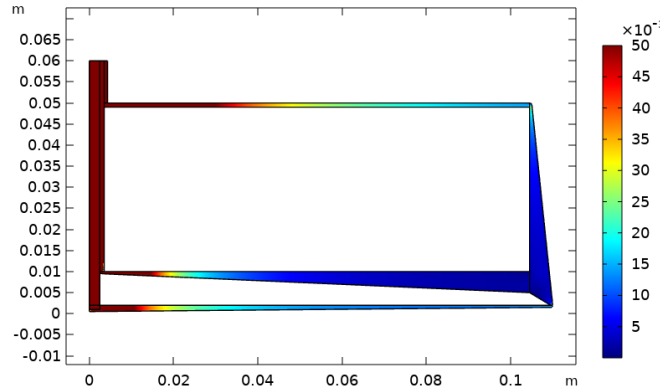
Figure 3.36 Velocity map of OC model #3 (unit: m/s).

3.5.3 Pressure and Shear Rate Analysis

The pressure (unit: Pascal) and shear rate (unit: 1/s) were different results in each case. Model #2 had excessively high pressure through the whole system (Figure 3.37). The three narrow areas might cause increased pressure. The OC models #1 and #3 had a similar trend, and #1 had less pressure in all locations.
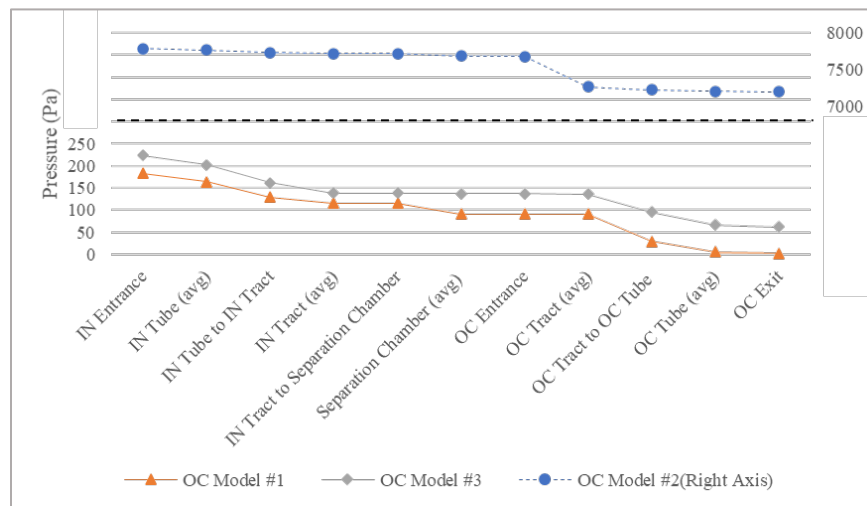
Figure 3.37 Pressure analysis in study 2-3.

A high shear rate was found in the narrow areas where the flow was accelerated and the OC tract and OC tube junction. The highest shear rate was recorded at the OC entrance

61

from the separation chamber. The round shape structures in model #3 reduced the shear rate (Figure 3.38).
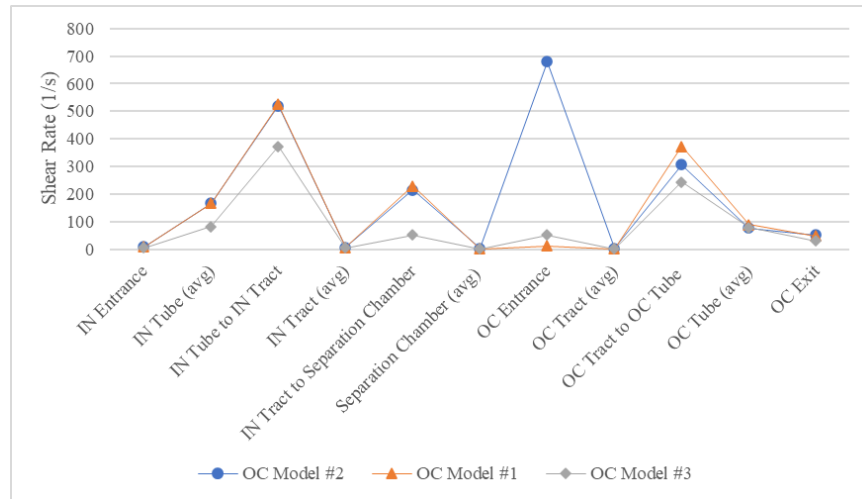
Figure 3.38 Shear rate analysis in study 2-3.

Chapter 4: Conclusion and Discussion

4.1 Conclusion

This research evaluated a centrifugal separator by computer simulation. Several hundred combinations of parameters were used to demonstrate and investigate separation efficiency. It was investigated in several variations of a Centritech Lab III type model and the new design models developed for this research.

For the purpose of the first research goal, a computer simulation model of an industry-standard Centritech Lab III centrifuge as a semi-continuous device was developed in study 1-1. This model moved cells downward by centrifugal force and could concentrate cells in the lower area of the bladder at least 3.5-fold in 10 minutes and 5.5 times in 30 minutes in a semi-continuous manner. The VF distribution differed by flow velocity. VF tended high in the lower area of the bladder with low flow velocity cases, and sedimentation near the inlet was found with the higher flow velocity. The computer simulation confirmed that this device was beneficial in cell separation for semi-continuous use.

For the second research goal, a Centritech Lab III centrifuge model for the continuous operation was developed in study 1-2. The model used an air barrier as a fixed interior wall to separate the bladder components for cell concentration and supernatant. As a result, however, cells settled as sediment on the interior wall or bottom wall by centrifuge, and any tested flow settings couldn't carry the cells from the inlet to the OC exit. The Centritech Lab III type centrifuge system couldn't be adapted for continuous operation.

For the third research goal, a developed model was used to characterize cellular separation in two novel centrifuge designs with respect to feasibility in study 2. The new models were created based on structure and media property tests. The new OC and No-OC models were tested. It was challenging to increase the cell concentration of the OC model because the OC route was directed backward in the direction of the centrifuge axis of rotation. VF for cell concentration tended to decrease when the flow velocity or rotation speed was unbalanced. After assembling the simulation model, reworking and additional tests were conducted in the creation process. Based on the theory of $F_d = F_{cfg}$, adjusting flow velocity was effective in reducing the VF difference between OC entrance and OC exit. Some OC model test cases, considered supernatant removal, allowed removing a high volume of supernatant without losing many cells.

The No-OC model yielded a greater cell concentration than the OC model and achieved high supernatant removal. These No-OC tests provided a possibility to effectively separate the cells from media with a benchtop size continuous operation device, though it needed to consider additional cell collection devices.

The flow velocity stability and the shear rate in the created model were assessed, and the high pressure and high shear rate were found in the narrow area of the models. The pressure and shear stress assessment should be evaluated in the actual demo devices in future research.

For real prototypes, media elements can be changed, but testing with many different structures is difficult and costly. Therefore, verification by computer simulation was considered to be meaningful. Since this study is a computer simulation, comparison and correction with the actual device will be the subject of future research.

4.2 Discussion

The findings of this computer simulation study suggested that it was possible to compare centrifuge models and geometries without making actual prototype devices or testing with real cells with a bioreactor. However, the result in study 2 showed some limitations regarding modeling cell collection, effective separation, and avoiding pelleting and shear stress. Also, there were some limitations in the methodology using computer simulation and CFD application.

4.2.1 Flow and Centrifuge Balance in Outlet Tract for Cell Collection

The expected direction of flow was different in OS and OC tracts though both tracts are parallel. This requirement made the model complicated. The centrifugal force and drag force affected the cells, and also, the pressure gradient and virtual mass force affected movement. These forces were differed by cell location in the devices and relative positions within structures such as walls. It was difficult to figure out the optimal centrifugal rotation speed and flow velocity by calculation. When calculating the balance between centrifugal force and drag force, an equation that removes buoyancy and gravity by assuming that the cell is at the terminal velocity was considered. Also, compensation for the influence of pressure gradient force by assuming that it was a perfect fluid was attempted. However, COMSOL simulations showed a difference from the assumption. Therefore, COMSOL Multiphysics was useful to calculate the influence that requested more tests necessary to eliminate the difference with theory.

While the OC model still had difficulty with flow back to the center even when balancing the forces to minimize the stagnation and lost cells, the result in study 2 showed

that the No-OC model had a much higher cell concentration and low lost cell rate. However, the No-OC model needs additional operations to collect the cells from the fast-moving rotating rotor, requiring clean environment operation or the closed system to prevent contamination. The cell collecting technology in the small size device will be an ongoing problem that should be overcome.

Methods to collect concentrated cells in the No-OC model should be considered. The first idea is that the cells are collected in the liquid. Centritech uses a polyurethane film bladder as a disposable. For the No-OC model of study 2-2, the unit is plastic sterile and used once, which has advantages for maintaining aseptic conditions. Other companies may be working on similar models. However, further studies are needed on actually collecting the cells from the separator and returning them to the bioreactor while preventing cell damage. Connection to a vessel or pump will be a practical issue that must be resolved.

4.2.2 Separation Efficiency and Centrifuge

The applied rotation of the centrifuge unit reached 2000 rpm or 3000 rpm in the set of testing with the No-OC tract model in study 2-2, and the centrifugal force overweighed other inward forces even with relatively high flow velocities. However, the cells are generally pelleted by centrifugation at 180 G or greater (Thermo Phisher, n.d.). This centrifuge model has an 11 cm radius disk and yields 180 G with 1200 rpm. 2000 rpm and 3000 rpm yield 491.92 G and 1106.82 G, respectively. One will have to test with real cells that do not exceed the gravitational force that results in pelleting for the used cells. Further study with an actual prototype demo device and microscopic examination will be required to confirm this possibility.

4.2.3 Velocity Control with Managing Shear Stress

In the velocity evaluation in study 2-3, OC model #2 had very high pressure and high shear stress in the narrow areas. At the same time, the narrow structure in this model gave an additional pump effect explained by Pascal's principle that increases the local flow velocity and the force to help the cells to move out from the separation chamber. I assumed this technique could be used in a closed flow circuit like this model, controlling the shear stress and damaging cell risk. Since this research was limited to the computer simulation, the demo testing with a prototype device would be helpful to figure out the critical point of pressure and shear stress with this model.

4.2.4 Test Protocol with Numerous Combination

The selected test items in this research were expected to affect the centrifugal pump. The set of simulations was performed by combining the parameters that gave better numerical outcome values for each test. However, there are many influential parameters in shape, flow, and centrifuge, and also they influence each other. For these reasons, it was difficult to converge on one model. The model specifications were selected based upon the output within the limits of the tested combinations.

If there are conflicting items, a trade-off curve may represent the relationship and find out the compromised point. In this study, a compromise between the centrifugal force and drag force by flow velocity in the OS tract reduces the number of lost cells from the OS in study2-2. However, testing with the $F_d = F_{cfg}$ method did not give the best results. The balance of these two forces or applied parameters was not good enough to consider the balance in the whole system. Kelly (2016) reported that the balance-aware setting was

effective for elutriation devices. Since the inlet and outlet are lined up in a straight line in their elutriation device, it might not be difficult to predict by combining the effect by F_d and F_{cfg}. The results might not be as calculated because my new OC model includes three in and out and the OS and OC positions are in a three-dimensional positional relationship.

Simulations were conducted using numerous combinations of variables to determine the specifications of the parts of the models investigated in this study. Once the actual working unit is created in the real world, the structure test can't be repeated easily, whereas the media property test can try different combinations. From this result, it seems that the prediction requires more complicated calculations and rationale. However, deciding the parameters to be tested after considering the balance between centrifugal force and drag force, which significantly affects the movement of the cell, seemed to be a more reasonable method than blindly selecting numerical values and proceeding with the test. Therefore, it is still helpful to perform computer simulations before the actual model test.

4.2.5 Limitation of Lagrangian Approach

COMSOL particle tracking interface is a useful tool to visualize each particle movement in the CFD models. This study used the particle tracking module in the early stage, but the multiphase interface was used instead because of the known difficulty of the Lagrangian approach's limitation. In this particle tracking interface, particles can't slide downward along the wall by continuous centrifugal application like figure 4.1. If a particle slides on a boundary, it interacts with the boundary infinite times, which is not tractable using the Lagrangian approach.
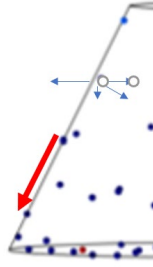
Figure 4.1 Repetitive wall interactions prevent particles slide along the wall.

According to COMSOL support, in some cases, refining the mesh and tightening the timesteps taken by the solver can help, but in this case, it was difficult for the particle tracing interface to handle. This issue is the current technology limitation, and the solution with other methods was necessary to model the physical phenomenon successfully.

4.2.6 Computing Difficulty in Complex Design

The more complex the model is, the more computational time is needed. Also, when the computing failed after waiting for the computer's calculation, the time would be wasted. If there is a complicated structure or a small calculation inconsistency on the model, it may continue running until it reaches the criteria to detect an error. At first, the 3D model was used for Centritech type model analysis in study 1. The 3D model in figure 4.2 was the design in the early stage of this study. They look not so complicated in structure. However, the model has a large 50 cm circumference with a 22 cm diameter, while the cell size is a small seven μm diameter.

Downscaling and miniaturing a model is a common method in computer simulation to reduce the computing load and time. However, the miniaturing technique wasn't used in this research because it could be difficult to find out how to check the miniatured model to align with the real size model. If the physical balance between cells and fluid would change

by downsizing, and the output results might differ from the original, the comparison with data from the actual machine's bench test result would be beneficial. The balance between the credibility and simplification of the model is essential, and so the simulation plan is constantly reviewed and flexibly changed if needed.
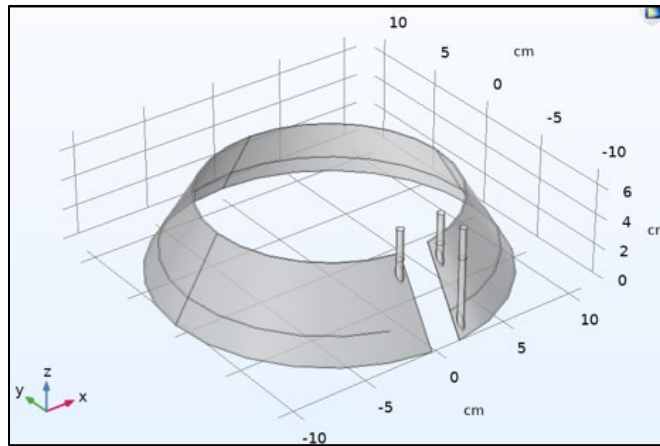
Figure 4.2 Centritech type culture 3D simulation model.

4.3 Future Study

Based on this computer simulation study result, an actual prototype centrifugal device will be made. The testing will determine if the prototype operates as predicted by the models, using latex beads and real cells. When there is cell damage or lower throughput than expected, models will be adjusted through additional simulations. The prototype will be integrated into the bioreactor system for comprehensive operation and performance testing.

References

Applikon Biotechnology. (n.d.). Cell culture perfusion. Retrieved from https://www.applikon-biotechnology.com/en/products/perfusion/biosep/

Clift, R., & Gauvin, W. H. (1971). Motion of entrained particles in gas streams. The Canadian Journal of Chemical Engineering, 49(4), 439-448. doi:10.1002/cjce.5450490403

COMSOL. (2020). CFD Module User's Guide 5.6. COMSOL

Dryden, W. A., Larsen, L. M., Britt, D. W., & Smith, M. T. (2021). Technical and economic considerations of cell culture harvest and clarification technologies. Biochemical Engineering Journal, 167, 107892. doi:10.1016/j.bej.2020.107892

Harrison, R. G. (2003). Bioseparations science and engineering. New York: Oxford University Press.

Janas, M., Nunes, C., Marenghi, A., Sauvage, V., Davis, B., Bajaj, A., Burns, A. (2015). Perfusion's Role in Maintenance of High-Density T-Cell Cultures. BioProcess International. 13. https://bioprocessintl.com/upstream-processing/bioreactors/perfusions-role-maintenance-high-density-t-cell-cultures/

Kelly, W., Rubin, J., Scully, J., Kamaraju, H., Wnukowski, P., & Bhatia, R. (2016). Understanding and modeling retention of mammalian cells in fluidized bed centrifuges. Biotechnology progress, 32(6), 1520–1530. https://doi.org/10.1002/btpr.2365

Kim, B. J., Oh, D. J., & Chang, H. N. (2008). Limited use of Centritech Lab II Centrifuge in perfusion culture of rCHO cells for the production of recombinant antibody. Biotechnology progress, 24(1), 166–174. https://doi.org/10.1021/bp070235f

Levine, B. L., Miskin, J., Wonnacott, K., & Keir, C. (2016). Global Manufacturing of CAR T Cell Therapy. Molecular therapy. Methods & clinical development, 4, 92–101. https://doi.org/10.1016/j.omtm.2016.12.006

Pneumatic Scale Angelus. (2018). Centritech Lab-III Operator's Manual, Rev.A.

Poon, C. (2020). Measuring the density and viscosity of culture media for optimized computational fluid dynamics analysis of in vitro devices. doi:10.1101/2020.08.25.266221

Shekhawat, L. K., Sarkar, J., Gupta, R., Hadpe, S., & Rathore, A. S. (2018). Application of CFD in Bioprocessing: Separation of mammalian cells using disc stack centrifuge during production of biotherapeutics. Journal of biotechnology, 267, 1–11. https://doi.org/10.1016/j.jbiotec.2017.12.016

Tasnim, H., Fricke, G. M., Byrum, J. R., Sotiris, J. O., Cannon, J. L., & Moses, M. E. (2018). Quantitative Measurement of Naïve T Cell Association With Dendritic Cells, FRCs, and Blood Vessels in Lymph Nodes. Frontiers in Immunology, 9. doi:10.3389/fimmu.2018.01571 https://www.frontiersin.org/articles/10.3389/fimmu.2018.01571/full#:~:text=A%20 na%C3%AFve%20T%20cell%20has,a%20pixel%20is%201.2%20%CE%BCm.

ThermoFisher Scientific. (n.d.). Primary Cell Culture Frequently Asked Questions. Retrieved from https://www.thermofisher.com/us/en/home/life-science/cell-culture/primary-cell-culture/primary-cell-culture-resources/frequently-asked-questions.html

Wang, Z., Wu, Z., Liu, Y., & Han, W. (2017). New development in CAR-T cell therapy. Journal of hematology & oncology, 10(1), 53. https://doi.org/10.1186/s13045-017-0423-1

Wu, M., Ozcelik, A., Rufo, J., Wang, Z., Fang, R., & Jun Huang, T. (2019). Acoustofluidic separation of cells and particles. Microsystems & nanoengineering, 5, 32. https://doi.org/10.1038/s41378-019-0064-3

Zipursky, A., Bow, E., Seshadri, R. S., & Brown, E. J. (1976). Leukocyte density and volume in normal subjects and in patients with acute lymphoblastic leukemia. Blood, 48(3), 361–371. https://pubmed.ncbi.nlm.nih.gov/1066173/#:~:text=The%20median%20cell%20den sities%20of,than%201.080%20g%2Fml).

Appendix A: Forces

A.1 Forces

In fluid dynamics, the movement of each particle follows Newton's equation of motion (second law). The total force on the particle F_t (SI unit: N) is given by

$$F_t = \frac{d}{d_t}(m_p \cdot v)$$

where m_p is the particle mass (SI unit: kg), v is the particle velocity (SI unit: m/s).

Drag force, optional virtual mass force, pressure gradient force are considered as forces that affect particle movement.

A.2 Drag Force

Stokes' law's drag force is a force that acts on an object moving or placed in the fluid toward the same direction as the flow velocity and opposite to the movement of the object. Drag force F_d (SI unit: N) in laminar flow is given by

$$F_d = 3\pi \cdot \mu \cdot d_p \cdot u$$

and F_d in turbulent flow is given by

$$F_d = C_d \cdot \frac{\rho}{2} \cdot u^2 \cdot \frac{\pi \cdot d_p^2}{4}$$

where u is the fluid velocity (SI unit: m/s), μ is the fluid dynamic viscosity (SI unit: Pa·s), d_p is the spherical particle diameter (SI unit: m), C_d is the drag coefficient, and ρ is the fluid density (SI unit: kg/m^3).

A.3 Virtual Mass Force

When a particle moving in a uniform flow accelerates, the fluid in the vicinity of the particle also accelerates. As a reaction, when a particle gives velocity to a fluid, the equivalent force that the particle receives from the fluid is the virtual mass force. Virtual mass force F_{vm} (SI unit: N) is given by

$$F_{vm} = \frac{1}{2} \cdot m_f \cdot \frac{d(u - v)}{dt}$$

where d/d_t is the material derivative in the direction of the particle velocity. m_f is the fluid mass displaced by the particle volume (SI unit: kg) derived from

$$m_f = \frac{1}{6} \cdot \pi \cdot d_p^3 \cdot \rho$$

where ρ is the fluid density.

A.4 Pressure Gradient Force

A pressure gradient force is a force per unit mass derived as the ratio of a pressure difference calculated by dividing by the distance over which the difference arises. Pressure gradient force F_{pg} (SI unit: N) is given by

$$F_{pg} = m_f \cdot \frac{D_u}{D_t}$$

where D/D_t is the material derivative in the direction of the fluid velocity.

A.5 Gravity Force

Gravity force F_g (SI unit: N) acts on particles and is given by

$$F_g = m_p \cdot \frac{g(\rho_p - \rho)}{\rho_p}$$

where g is the gravity vector (SI unit: m/s²) at sea level g = 9.80665 (m/s²), and ρ_p is the particle density (SI unit: kg/m³).

A.6 Centrifugal Force

When it is rotated, a centrifugal force arises as to the apparent outward force on a mass. The centrifugal force is very real for the objects in the rotating frame. It causes them in a rotating frame of reference to give accelerating outward from the center of rotation. Centrifugal force F_{Cfg} (SI unit: N) is given by

$$F_{cfg} = m \cdot \omega^2 \cdot R$$

$$= \frac{1}{6} \cdot \pi \cdot d_p^{\,3} \cdot (\rho_p - \rho) \cdot \omega^2 \cdot R$$

where m is the mass (SI unit: kg), ω is the angular velocity (SI unit: rad/s), and R is the distance of the particle from the center of rotation (radius of revolution, SI unit: m).

The velocity v_{cfg} in the centrifugal field is given by

$$v_{cfg} = \frac{d_p^{\,2}(\rho_p - \rho)\omega^2 \cdot R}{18 \cdot \mu}$$

called the centrifuge equation.

A.7 Centrifugal Effect as G Force

The centrifugal effect increases proportionally to the number of revolutions and the radius of the revolution. Relative centrifugal force (RCF) [×g] is given by

$$RCF = 1.118 \cdot 10^{-5} \cdot N^2 \cdot r$$

where N is the number of revolutions [rpm], and r is the radius of revolution [cm].

For instance, when the rotor revolves at 100 rpm and the radius is 10cm, as the angular velocity is 10.48 rad/s, the G force is 1.18 G.

Appendix B: Flow Velocity and Flow Volume

B.1 Inlet Flow Velocity and Volume Flow Rate

The total volume flow rate is derived from the inlet flow velocity and the inlet cross-sectional area. This model's cross-sectional area is 0.196 cm^2 with a diameter of 0.5 cm.

Table B.1 Inlet flow velocity and total volume flow rate.

		Inlet Flow Velocity (m/sec)				
		0.04	0.08	0.16	0.32	0.48
Volume Flow Rate	(ml/sec)	0.79	1.57	3.14	6.28	9.42
	(ml/min)	47.12	94.25	188.50	376.99	565.49
	(l/hour)	2.83	5.65	11.31	22.62	33.93

B.2 OC and OS Flow Velocity with OC Ratio

OC (Concentration) and OS (Supernatant) change by OC ratio. Table B.2 and B.3 show the OC and OS flow velocity and volume flow rate when the inlet flow velocity of 0.16 m/s and 0.48 m/s.

Table B.2 OC and OS flow at inlet flow 0.16 m/s.

Inlet Flow 0.16 m/s		OC Ratio				
		0.1	0.25	0.5	0.75	0.9
OC Flow	Velocity (m/s)	0.016	0.040	0.080	0.12	0.14
	Volume (ml/s)	0.31	0.79	1.57	2.36	2.83
OS Flow	Velocity(m/s)	0.14	0.12	0.080	0.040	0.016
	Volume (ml/s)	2.83	2.36	1.57	0.79	0.31

Table B.3 OC and OS flow at inlet flow 0.48 m/s.

Inlet Flow		OC Ratio				
0.48 m/s		0.1	0.25	0.5	0.75	0.9
OC Flow	Velocity (m/s)	0.048	0.12	0.24	0.36	0.43
	Volume (ml/s)	0.94	2.36	4.71	7.07	8.48
OS Flow	Velocity (m/s)	0.43	0.36	0.24	0.12	0.048
	Volume (ml/s)	8.48	7.07	4.71	2.36	0.94

Appendix C: List of Abbreviations

C.1 Abbreviations

Table C.1 is the list of abbreviations used in this research.

Table C.1 List of abbreviations.

ATF	Alternating tangential flow filtration
CAR	Chimeric antigen receptor
C_d	Drag coefficient
CFD	Computational fluid dynamics
CIP	Clean-in-place
FBS	Fetal bovine serum
F_{cfg}	Centrifugal force
F_d	Drag force
FEM	Finite element method
HARV	High aspect ratio vessel
IN	Inlet (for feed)
No-OC	No outlet for cell concentration
OC	Outlet for cell concentration
OS	Outlet for supernatant
RANS	Reynolds-averaged Navier–Stokes
SIP	Steam-in-place
TFF	Tangential flow filtration
VF	Volume fraction